motif. In the case of Uba5, the Cys^{250} seems to be the most possible active site Cys residue (Figure 1B). If an active site Cys residue within an E1 and E1-like enzymes is changed to Ser, an O-ester bond instead of a thioester bond is formed with its respective modifier protein and the intermediates become stable even under reducing conditions. Therefore, we mutated Cys^{250} within Uba5 to Ser and expressed it as a Flag-fused $Uba5^{C250S}$ (Flag-$Uba5^{C250S}$) or Flag-Uba5 as control in HEK293 cells. As shown in Figure 1C, both Flag-Uba5 and Flag-$Uba5^{C250S}$ were expressed as ~50 kDa proteins in HEK293 cells. When Flag-$Uba5^{C250S}$ was expressed, an additional band with a higher molecular mass of ~60 kDa was clearly observed, indicating that Flag-$Uba5^{C250S}$ forms an intermediate complex with an endogenous protein. These results suggest that Uba5 is indeed a novel protein-activating enzyme for a presumptive modifier (see below).

Identification of a novel ubiquitin-fold molecule, Ufm1

Because Uba5 was identified as GATE-16-binding protein, we initially assumed that Uba5 is another GATE-16-activating enzyme, in addition to Atg7. To test this possibility, we examined whether $Uba5^{C250S}$ (the presumptive active site Cys at position 250 was replaced by Ser) forms an intermediate complex with GATE-16 or not. Unexpectedly, we could not identify a stable complex between $Uba5^{C250S}$ and GATE-16 (data not shown). Therefore, we attempted to identify a protein(s) that physically associates with Uba5 in the cells. To do this, Flag-Uba5 was expressed in HEK293 cells, then immunoprecipitated by anti-Flag antibody. The immunoprecipitates were eluted with a Flag peptide, then digested with Lys-C endopeptides (*Achromobacter* protease I) and the cleaved fragments were directly analyzed using a highly sensitive 'direct nano-flow LC–MS/MS' system as described in Materials and methods. Following database search, a total of 28 peptides were assigned to MS/MS spectra obtained from four nano-LC–MS/MS analyses for the Flag-Uba5-associated complexes. These peptide data identified three proteins as Uba5-associated components: GATE-16, and hypothetical proteins BM-002 and CGI-126 (excluding the bait protein Uba5 and the background proteins, such as HSP70 and keratins).

One of these identified proteins, BM-002, is an 85-amino-acid protein with a predicted molecular mass of ~9.1 kDa. This protein is conserved in multicellular organisms, but not in yeasts, like Uba5 (Figure 2A). The human BM-002 has high identity over the species in the central region but has elongated sequences at both N- and C-terminal regions in some species. Although the protein shows no clear overall sequence identity to ubiquitin or other modifiers (Figure 2B), the tertiary structure of BM-002 displays a striking resemblance to human ubiquitin (Figure 2C). The human structure of BM-002 was constructed by a computer-assisted modeling, based on the structure of its *C. elegans* homolog that has been analyzed previously, as a protein possessing 'ubiquitin-like fold' with secondary structure elements ordered β–β–α–β–β–α (α-helix and β-sheet) along the sequence (Cort *et al*, 2002). Thus, we named human BM-002 as Ufm1.

Ubiquitin is synthesized in a precursor form that must be processed by de-ubiquitylating enzymes (DUBs) to generate a Gly–Gly sequence at the C-terminus. Similarly, Ufm1 has a single Gly residue conserved across species at the C-terminal region, although the length and sequences of amino acids extending from this Gly residue vary among species. To test whether the C-terminus of Ufm1 is post-translationally cleaved, we constructed an expression vector for Ufm1 tagged at both the N- and C-ends, that is, a Flag epitope at the N-terminus and an HA epitope at the C-terminus (Flag-Ufm1-HA) (Figure 2D). After transfection of Flag-Ufm1-HA into HEK293 cells, the cell lysate was subjected to SDS–PAGE, and Flag-Ufm1-HA was detected by immunoblotting. A 10-kDa protein corresponding to Ufm1 was recognized with anti-Flag antibody, while no appreciable protein was observed with anti-HA antibody (Figure 2E, lanes 2 and 7). The mobility on SDS–PAGE was similar to that of Flag-Ufm1ΔC2 (equivalent to mature $Ufm1^{1-83}$ protein) lacking the C-terminal Ser^{84} and Cys^{85} of proUfm1 (Figure 2E, lane 4). These results suggested that the C-terminus of Ufm1 is post-translationally cleaved in the cells, producing mature Ufm1 with the C-terminal Gly^{83} residue. It is known that the replacement of C-terminal Gly residue of Ub and other UBLs with an Ala residue inhibits the C-terminal processing (Kabeya *et al*, 2000; Tanida *et al*, 2003). To examine whether Gly^{83} of Ufm1 is essential for the cleavage, Gly^{83} of Flag-Ufm1-HA was mutated to Ala, and expressed in HEK293 cells (Figure 2D, Flag-$Ufm1^{G83A}$-HA). The mobility of most Flag-$Ufm1^{G83A}$-HA on SDS–PAGE was apparently slower than that of Flag-Ufm1-HA (Figure 2E, lane 3). This mutant was recognized by immunoblotting with anti-HA antibody as well as anti-Flag antibody, suggesting that mutation Gly^{83} to Ala confers resistance to its C-terminal cleavage.

Uba5 is an Ufm1-activating enzyme

We next investigated whether Uba5 forms an intermediate complex with Ufm1. We expressed Flag-Uba5 or Flag-$Uba5^{C250S}$ with Myc-tagged Ufm1 (Myc-Ufm1) in HEK293 cells. Myc-tagged Ufm1ΔC3 lacking the C-terminal Gly^{83} of mature Ufm1 (Myc-Ufm1ΔC3; i.e., deletion form of three residues from precursor $Ufm1^{1-85}$ protein) was used as control. Each cell lysate was prepared and analyzed by immunoblotting with anti-Flag antibody. Flag-$Uba5^{C250S}$ formed an intermediate with an endogenous protein as shown in Figure 1 (Figure 3A, lane 7). When Flag-$Uba5^{C250S}$ was coexpressed with Myc-Ufm1, the intermediate shifted to higher molecular weight (Figure 3A, lane 8). The higher band was not detected when Myc-Ufm1ΔC3 was coexpressed (Figure 3A, lane 9). To verify that the intermediate is indeed the Uba5–Ufm1 complex, Flag-$Uba5^{C250S}$ was immunoprecipitated and blotted with anti-Flag and anti-Myc antibody. Consistent with the above data, a higher sized intermediate was observed when Flag-$Uba5^{C250S}$ was coexpressed with Myc-Ufm1 (Figure 3B, top panel, lane 5), but not alone or with Myc-Ufm1ΔC3 (Figure 3B, top panel, lanes 4 and 6). The intermediate was also recognized by anti-Myc antibody (Figure 3B, lower panel, lane 5), indicating the existence of the Flag-$Uba5^{C250S}$–Myc-Ufm1 complex. Note that the small-sized intermediate is presumably a complex with an endogenous Ufm1, as mentioned. These results indicate that Uba5 forms an intermediate with Ufm1 and the Gly^{83} residue of Ufm1 is essential for the formation of the intermediate with Uba5 *in vivo*.

We subsequently tested whether Uba5 can activate Ufm1 *in vitro*. The thioester formation assay was performed using recombinant proteins expressed in *Escherichia coli*. Recombinant GST-tagged Uba5 and mature Ufm1

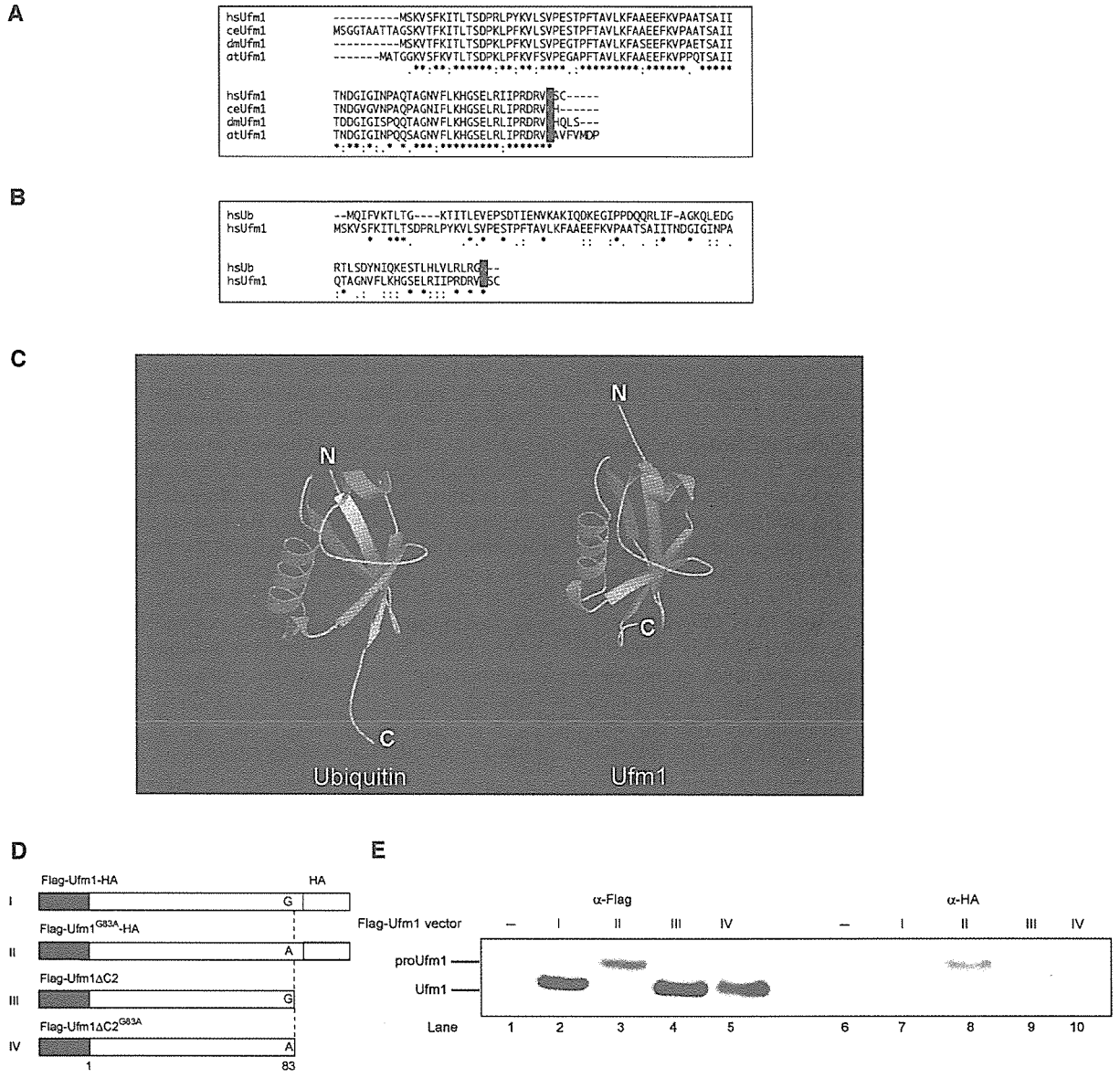

Figure 2 Ufm1, a novel ubiquitin-fold molecule. (**A**) Sequence alignment of hsUfm1 and its homologs. The sequence of hsUfm1 is available from GenBank^{TM} under the accession number BC005193 (dm, a coding region of dmUfm1 was found from *D. melanogaster* genomic sequence; ce, NM_066304; at, NM_106420). The homology analysis was performed as described in Figure 1B. The C-terminal conserved Gly residue is boxed in black. (**B**) Sequence alignment of hsUbiquitin with hsUfm1. The homology analysis was performed as described in Figure 1B. The C-terminal conserved Gly residue is boxed in black. (**C**) Structural ribbon of hsUbiquitin and predicted structural ribbon of hsUfm1. α-Helices and β-strands are shown in green and yellow, respectively. The homology model of hsUfm1 was created from the *C. elegans* Ufm1 structure (Cort *et al*, 2002) by using MOE program (2003.02; Chemical Computing Group Inc., Montreal, Quebec, Canada). (**D**) Schematic representation of mammalian expression plasmids for Ufm1 and the derivative mutants. Flag epitope tags at the N-terminus, HA epitope tags at the C-terminus, and putative cleavage site Gly^{83} residue (vertical dotted lines) are indicated. To construct Ufm1^{G83A}, a single point mutation was introduced into Ufm1, which led to an amino-acid substitution from Gly to Ala at position 83. To construct Ufm1ΔC2, the two C-terminal residues were deleted by PCR. Ufm1ΔC2^{G83A} was also produced by site-directed mutagenesis of Ufm1ΔC2. The ΔC2 mutants were tagged with the Flag epitopes at N-terminus. (**E**) ProUfm1 processing. HEK293 cells were transfected with Flag-Ufm1-HA, Flag-Ufm1^{G83A}-HA, Flag-Ufm1ΔC2, or Flag-Ufm1ΔC2^{G83A}. The cell lysates were subjected to SDS–PAGE and analyzed by immunoblots with anti-Flag and anti-HA antibodies. ProUfm1 and mature Ufm1 are indicated on the left. The numbers at the top from I to IV are similar to those in (D).

(Ufm1ΔC2) with exposed C-terminal Gly^{83} residue were purified, mixed and incubated in the presence of ATP and then subjected to SDS–PAGE at either reducing or nonreducing conditions. GST-Ufm1ΔC3 was used as control. An ~100 kDa band corresponding to the GST-Ufm1ΔC2–GST-Uba5 intermediate complex was clearly observed when the mixture was applied at nonreducing conditions (Figure 3C, lane 3). This intermediate was not observed when ATP or GST-Uba5 was excluded from the mixture (Figure 3C, lanes 1 and 2), or when the mixture was loaded in the presence of

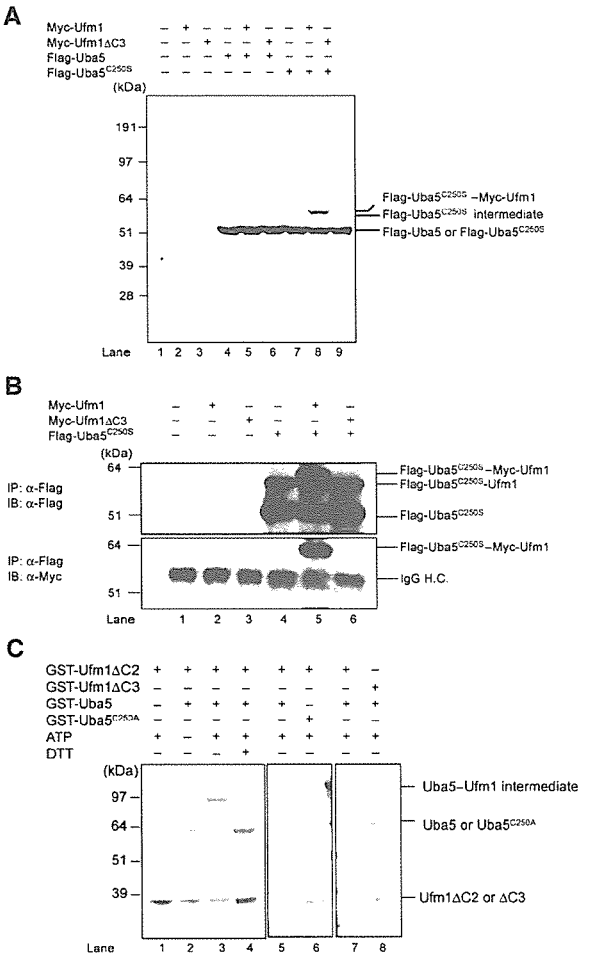

Figure 3 Demonstration that Uba5 is an Ufm1-activating enzyme. (**A**) Immunoblotting analysis. Each Myc-tagged Ufm1 (Myc-Ufm1) and Myc-Ufm1ΔC3 was expressed alone (lanes 2 and 3, respectively), and coexpressed with Flag-Uba5 (lanes 5 and 6, respectively) or Flag-Uba5^{C250S} (lanes 8 and 9, respectively). Each Flag-Uba5 and Flag-Uba5^{C250S} was also expressed alone (lanes 4 and 7, respectively). The cell lysates were subjected to SDS–PAGE and analyzed by immunoblotting with anti-Flag antibody. The bands corresponding to Flag-Uba5, Flag-Uba5^{C250S}, and Flag-Uba5^{C250S} intermediates are indicated on the right. (**B**) Immunoblotting analysis after immunoprecipitation. Each Myc-Ufm1 and Myc-Ufm1ΔC3 was expressed alone (lanes 2 and 3, respectively), and coexpressed with Flag-Uba5^{C250S} (lanes 5 and 6, respectively). Flag-Uba5^{C250S} was also expressed alone (lane 4). The cell lysates were immunoprecipitated with anti-Flag antibody. The resulting immunoprecipitates were subjected to SDS–PAGE and analyzed by immunoblotting with anti-Flag and anti-Myc antibodies. The bands corresponding to Flag-Uba5^{C250S}, Flag-Uba5^{C250S}–endogenous Ufm1, and Flag-Uba5^{C250S}–Myc-Ufm1 intermediates are indicated. (**C**) *In vitro* activating assay of Ufm1 by Uba5. Purified recombinant GST-Ufm1ΔC2 (2 μg) (lanes 1–7) was incubated for 30 min at 25°C with some of the following: 2 μg of purified recombinant GST-Uba5 (lanes 2–5, 7, and 8), GST-Uba5^{C250A} (lane 6), and 5 mM ATP (lanes 1 and 3–8). Lane 8 was conducted similar to lane 7, except that GST-Ufm1ΔC3 was used instead of GST-Ufm1ΔC2. Reactions were then incubated with SDS loading buffer lacking reducing agent (lanes 1–3 and 5–8) or containing 100 mM DTT (lane 4). The presence or absence of various components is indicated above the lanes. The bands corresponding to free GST-Uba5, GST-Uba5^{C250A}, GST-Ufm1ΔC2 (mature Ufm1), GST-Ufm1ΔC3, and GST-Uba5–GST-Ufm1ΔC2 thioester product are indicated on the right.

a reducing agent dithiothreitol (DTT) (Figure 3C, lane 4). Furthermore, GST-tagged Uba5^{C250A} mutant, a presumptive active site Cys mutant, could not form the intermediate even at nonreducing conditions (Figure 3C, lane 6). GST-tagged Ufm1ΔC3 was also incapable of forming the intermediate in this reaction (Figure 3C, lane 8). Taken together, we concluded that Uba5 is an Ufm1-activating enzyme and has the active site in Cys^{250}.

Identification of a novel protein-conjugating enzyme, Ufc1

The LC–MS/MS analysis revealed CGI-126 protein as another Uba5 interacting protein. CGI-126 is a protein of 167-amino-acid residues with a predicted molecular mass of 19.4 kDa. This protein is also conserved in multicellular organisms, like Uba5 and Ufm1 (Figure 4A). The C-terminal half of human CGI-126 has a high identity across species as shown in Figure 4A. CGI-126 has a highly conserved region, for example, residues 113–126, with limited similarity to the region of Ubc's that encodes an active site Cys residue capable of forming a thioester bond (Figure 4A). We assumed that this protein may be an E2-like conjugating enzyme for Ufm1 and thus named it Ufm1-conjugating enzyme 1 (Ufc1). If Ufc1 is an authentic E2 enzyme for Ufm1, it is expected to form an intermediate complex with Ufm1 via a thioester linkage. To test this possibility in the same way as Uba5, we mutated the predicted active site Cys residue within Ufc1 (Figure 4A, Cys^{116}) to Ser. We expressed Flag-Ufc1 or Flag-Ufc1^{C116S} (a presumptive active site Cys at position 116 was replaced by Ser) in combination with Myc-Ufm1 or Myc-Ufm1ΔC3 in HEK293 cells. Flag-Ufc1^{C116S} formed a stable intermediate band when coexpressed with Myc-Ufm1 (Figure 4B, lane 8), but not alone or with Myc-Ufm1ΔC3 (Figure 4B, lanes 7 and 9). To ascertain that this is the Flag-Ufc1^{C116S}–Myc-Ufm1 intermediate, Flag-Ufc1^{C116S} was immunoprecipitated and blotted with anti-Myc antibody (Figure 4C). Indeed, Myc-Ufm1, but not Myc-Ufm1ΔC3, formed a complex with Flag-Ufc1^{C116S} (Figure 4C, lanes 5 and 6, top and bottom panels). Note that Flag-Ufc1^{C116S} intermediate with a faster electrophoretic mobility than the Flag-Ufc1^{C116S}–Myc-Ufm1 complex is presumably the intermediate with the endogenous Ufm1 (Figure 4C, lanes 4–6, upper panel). These results indicate that Ufc1 forms an intermediate with Ufm1 *in vivo*.

To confirm that Ufc1 is indeed an E2-like enzyme that conjugates with Ufm1 *via* a thioester linkage, we conducted an *in vitro* Ufm1 conjugation assay. Recombinant GST-Uba5, GST-Ufc1, and GST-Ufm1ΔC2 were mixed and incubated in the presence of ATP. GST-Ufc1^{C116A} mutant and GST-Ufm1ΔC3 were used as negative controls. Under nonreducing conditions, an ~70 kDa band corresponding to GST-Ufm1ΔC2–GST-Ufc1 intermediate was observed (Figure 4D, lane 4). This product was not formed at reducing conditions, or when any of the components was omitted from the reaction (Figure 4D, lanes 1–3 and 5). GST-tagged Ufc1^{C116A} mutant could not form the intermediate, suggesting that Cys116 is indeed the active site (Figure 4D, lane 7). GST-Ufm1ΔC3 was again unable to form the intermediate complex in this reaction (Figure 4D, lane 9). Taken together, we concluded that Ufc1 functions as an Ufm1-conjugating enzyme and has the active site in Cys^{116}.

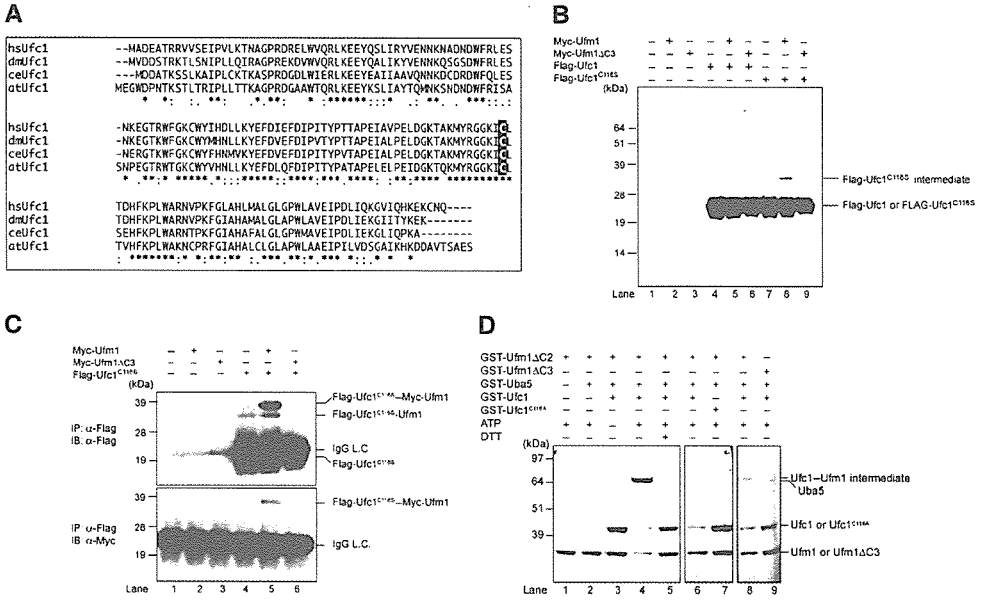

Figure 4 Ufc1, a novel E2-like enzyme. (**A**) Sequence alignment of hsUfc1 and its homologs. The sequence of Ufc1 is available from GenBank™ under the accession number BC005187 (dm, NM_137230; ce, NM_066654; at, BT001180). The homology analysis was performed as described in Figure 1B. The putative active site Cys residue is boxed in black. (**B**) Immunoblotting analysis. Each Myc-tagged Ufm1 (Myc-Ufm1) and Myc-Ufm1ΔC3 was expressed alone (lanes 2 and 3, respectively), and coexpressed with Flag-Ufc1 (lanes 5 and 6, respectively) or Flag-Ufc1^{C116S} (lanes 8 and 9, respectively). Each Flag-Ufc1 and Flag-Ufc1^{C116S} was also expressed alone (lanes 4 and 7, respectively). The cell lysates were subjected to SDS–PAGE and analyzed by immunoblotting with anti-Flag antibody. The bands corresponding to Flag-Ufc1, Flag-Ufc1^{C116S}, and Flag-Ufc1^{C116S} intermediates are indicated on the right. (**C**) Immunoblotting analysis after immunoprecipitation. Each Myc-Ufm1 and Myc-Ufm1ΔC3 was expressed alone (lanes 2 and 3, respectively), and coexpressed with Flag-Ufc1^{C116S} (lanes 5 and 6, respectively). Flag-Ufc1^{C116S} was also expressed alone (lane 4). The cell lysates were immunoprecipitated with anti-Flag antibody. The resulting immunoprecipitates were subjected to SDS–PAGE and analyzed by immunoblots with anti-Flag and anti-Myc antibodies. The bands corresponding to Flag-Ufc1^{C116S}, Flag-Ufc1^{C116S}–endogenous Ufm1, and Flag-Ufc1^{C116S}–Myc-Ufm1 intermediates are indicated. (**D**) *In vitro* thioester bond formation assay of Ufm1 by Ufc1. Purified recombinant GST-Ufm1ΔC2 (2 μg) (lanes 1–8) was incubated for 30 min at 25°C with the following: purified recombinant GST-Uba5 (0.2 μg) (lanes 2–9), GST-Ufc1 (2 μg) (lanes 3–6, 8, and 9), GST-Ufc1^{C116S} (2 μg) (lane 7), and 5 mM ATP (lanes 1, 2, and 4–9). Lane 9 was conducted similar to lane 8, except that GST-Ufm1ΔC3 was used instead of GST-Ufm1ΔC2. Reactions were then incubated with SDS loading buffer lacking reducing agent (lanes 1–4 and 6–9) or containing 100 mM DTT (lane 5). The presence or absence of various components is indicated above the lanes. The bands corresponding to free GST-Ufm1ΔC2 (mature Ufm1), GST-Ufm1ΔC3, GST-Uba5, GST-Ufc1, GST-Ufc1^{C116S}, and GST-Ufc1–GST-Ufm1ΔC2 thioester product are indicated on the right.

Conjugation of Ufm1 to cellular protein(s)

We next examined whether Ufm1 conjugates to the target protein(s) in cells. To this end, we expressed Flag- and 6xHis-tagged Ufm1 constructs in HEK293 cells, and purified them under denaturing conditions by Ni^{2+} beads. The resulting precipitates were then analyzed by immunoblotting with anti-Flag antibody. When FlagHis-Ufm1-HA (proUfm1) or FlagHis-Ufm1ΔC2 (mature form) was expressed, several proteins with sizes of about 28, 38, and 47 kDa were detected, in addition to the 10 kDa corresponding to free FlagHis-Ufm1ΔC2 (Figure 5A, lanes 2 and 4). These bands were not detected by FlagHis-Ufm1^{G83A}-HA and FlagHis-Ufm1ΔC3, suggesting that both C-terminal cleavage and C-terminal Gly residue are required for the conjugation reaction (Figure 5A, lanes 3 and 6). Moreover, these protein bands were resistant to reducing agents, such as DTT and β-mercaptoethanol. These results indicate that Ufm1 is covalently attached to some target proteins, probably through an isopeptide bond between the C-terminal Gly^{83} of Ufm1 and a Lys residue in the cellular proteins. It is of note that FlagHis-Ufm1^{G83A} mutant with exposed C-terminal Ala instead of Gly can conjugate to target proteins (Figure 5A, lane 5), consistent with the previous report on ubiquitin and SUMO (Hodgins *et al*, 1992; Kamitani *et al*, 1997). Since C-terminal Gly to Ala mutation confers resistance to the Ufm1 processing, the conjugates with FlagHis-Ufm1^{G83A} mutant may be more stable than those with FlagHis-Ufm1ΔC2 (Figure 5A, compare lanes 4 and 5). These results suggest that the Ufm1 conjugation is also a reversible reaction.

We further investigated the expression of Ufm1 and its conjugated proteins in mouse tissues using anti-Ufm1 serum. Ufm1 was widely expressed in all tissues examined, such as brain, heart, lung, liver, and kidney (Figure 5B, left panel). In addition, several bands with striking similarity to proteins detected in HEK293 cells were observed. These bands were not detected by preimmune or preabsorbed antisera (Figure 5B, right panel), suggesting that they are likely the Ufm1 conjugates. Although the intensity of each band varied among tissues and HEK293 cells, 28 and 38 kDa proteins were commonly detected. The 70-kDa band observed in all tissues was also detected faintly in HEK293 cells (Figure 5A, lane 5). The 47-kDa band observed in HEK293 cells was not clear. These protein bands were resistant to reducing agents, such as DTT and β-mercaptoethanol, indicating that Ufm1 covalently attaches to cellular proteins like other Ubl proteins. The targets of Ufm1 appeared to be common in a variety

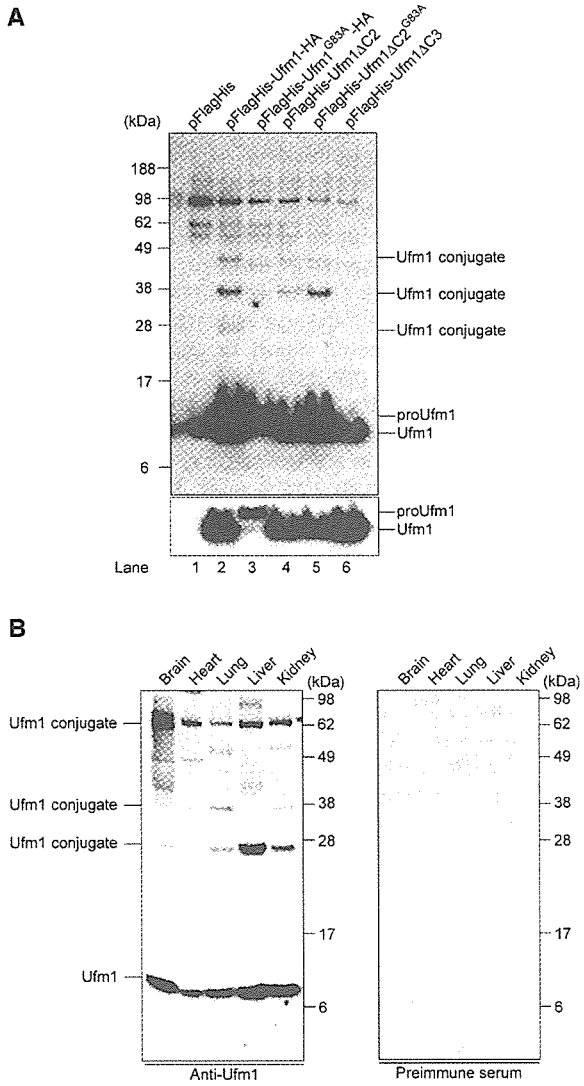

Figure 5 Formation of a covalent protein conjugate(s) with Ufm1 in HEK293 cells and mouse tissues. (**A**) Ufm1 conjugates in human HEK293 cells. HEK293 cells were transfected with FlagHis-Ufm1-HA, FlagHis-Ufm1^{G83A}-HA, FlagHis-Ufm1ΔC2, FlagHis-Ufm1ΔC2^{G83A}, or FlagHis-Ufm1ΔC3 expression plasmids. These cells were lysed under denaturing conditions, and the lysates were precipitated with Ni^{2+} beads. The precipitates were subjected to SDS–PAGE and analyzed by immunoblotting with anti-Flag antibody. The bottom panel shows the short exposure of the upper panel. The bands corresponding to mature Ufm1, proUfm, and Ufm1 conjugates are indicated on the right. (**B**) Ufm1 conjugates in various mouse tissues. Homogenates from mouse tissues as indicated were prepared and subjected to SDS–PAGE and analyzed by immunoblotting with anti-Ufm1 serum (left panel) or preimmune serum (right panel). The bands corresponding to Ufm1 and conjugates between Ufm1 and target proteins are indicated on the left.

of tissues. These results suggest the universal roles of Ufm1 in the regulation of cellular function in multicellular organisms.

Subcellular localization of Ufm1 in HeLa cells

We finally examined the subcellular distribution of Ufm1 in HeLa cells. Immunocytochemical analysis using anti-Ufm1

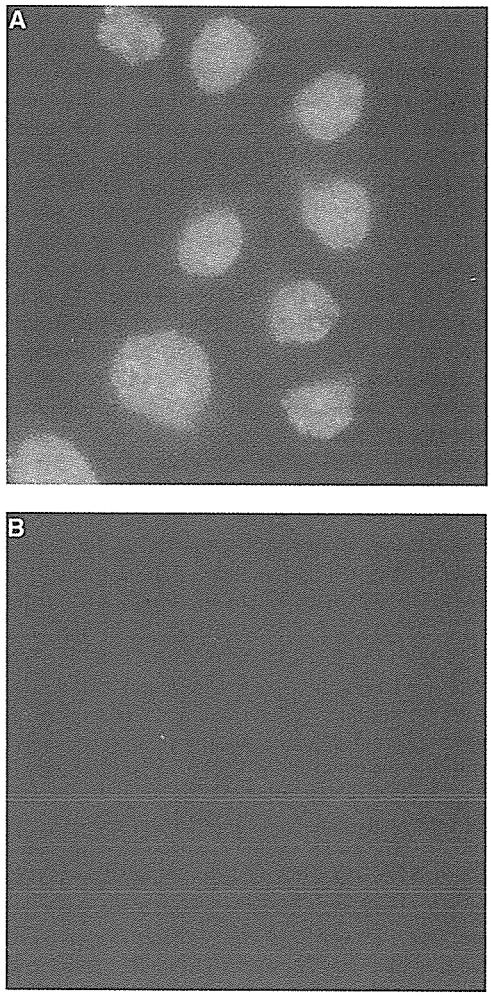

Figure 6 Intracellular distribution of Ufm1 in HeLa cells. (**A**) HeLa cells were seeded on coverslips 24 h before fixation for immunostaining. Ufm1 was detected with anti-Ufm1 serum and visualized with Alexa 488 nm anti-rabbit antibody. (**B**) Immunocytochemical analysis was conducted as for (A), except that preimmune serum was used. Cells were observed using a fluorescence microscope. Magnification, × 400.

serum revealed that Ufm1 was predominantly localized in the nucleus and diffusely in the cytoplasm (Figure 6A). These staining patterns were not observed when anti-Ufm1 serum had been preadsorbed with excess amounts of recombinant Ufm1 protein or preimmune serum was used instead of anti-Ufm1 serum (Figure 6B). Moreover, Ufm1 localization in the cytoplasm and nucleus was similar to the localization of exogenously expressed GFP-tagged Ufm1 in HeLa cells (data not shown). In the nucleus, strong immunoreactivity to anti-Ufm1 serum was observed as a dot-like structure. Although such dots-like structures were detected by preimmune serum, those intensities were weak. Thus, some of these dot-like structures may represent conjugates of Ufm1.

Discussion

In the present study, we reported that Ufm1 acts as a new post-translational UBL modifier, based on the following

criteria: (1) It is a small protein of 9.1 kDa with a ubiquitin-fold structure. (2) Ufm1 is synthesized in a precursor form, and the extra amino-acid residues at the C-terminal side need to be processed to expose the Gly residue. (3) The C-terminal processing and exposure of glycine residue are essential to the formation of Ufm conjugates in the cells. (4) Ufm1 has specific E1-like (Uba5) and E2-like (Ufc1) enzymes for activation and conjugation, respectively. Intriguingly, many UBL modifiers are evolutionarily conserved from yeast to human, except interferon-inducible UBL modifiers, such as UCRP/ISG15, Fat10, and Fau1/MNSFβ (Nakamura *et al*, 1995; D'Cunha *et al*, 1996; Liu *et al*, 1999). Ufm1, Uba5, and Ufc1 found in the present study are conserved in various multicellular organisms (Figures 1B, 2A, and 4A), but not in both budding and fission yeasts, suggesting that they all have been generated by coevolution.

We identified Uba5 as an E1 enzyme for Ufm1. This enzyme is relatively small compared to Uba1, that is, an E1 for ubiquitin (Figure 1A). In the *in vitro* assay, the recombinant Uba5 protein formed a thioester linkage with recombinant Ufm1 (Figure 3C) and transferred the activated Ufm1 to recombinant Ufc1 (an E2 enzyme) (Figure 4D), indicating that Uba5 can activate Ufm1 as a single molecule. This is in marked contrast to other E1s such as Uba2 and Uba3, which retain obvious similarities to the C-terminal half of Uba1 but require the formation of heterodimer complexes with respective partner molecules, AOS1 and APP-BP1, respectively, with similarities to the N-terminal half of Uba1 (Johnson *et al*, 1997; Liakopoulos *et al*, 1998; Osaka *et al*, 1998). Another E1-like enzyme, Uba4 that activates Urm1, is of similar size to Uba5 (Furukawa *et al*, 2000), but it remains unknown whether Uba4 acts as a single molecule or needs a partner subunit. The homology of Uba5 to Uba1 is less than those of Uba2 and Uba3, except their ThiF domain conserved in E1s, and thus it is likely that Uba5 may uniquely activate Ufm1, differing from other E1s such as Uba1, Uba2/AOS1, and Uba3/APP-BP1. Thus, although the structure of APP-BP1/Uba3 heterodimer is determined and the mechanism by which E1s activate their cognate UBLs was proposed (Walden *et al*, 2003a, b), the weak homology of Uba5 with other E1s hampered the computer-assisted structural analysis. To clarify this issue, structural analysis of Uba5 is required. This issue is currently under investigation in our laboratories. So far, most E1-like enzymes activate single species of UBL protein, although Atg7 is exception, which can activate both Atg8 and Atg12 (Mizushima *et al*, 1998; Tanida *et al*, 1999; Ichimura *et al*, 2000). A total of 10 E1-like enzymes can be identified in the human genome by computer analysis. Considering the limited number of E1-like proteins, it is possible that some E1-like proteins can activate a distinct set of UBL proteins. Whether or not Uba5 is capable of activating proteins other than Ufm1 remains to be clarified.

There are more than a dozen of E2 family genes in human genomes. In the budding yeast, 13 different E2s, namely Ubc1–Ubc13, have been documented and functionally characterized. Functionally, most of them catalyze the conjugation of ubiquitin, except that Ubc9 and Ubc12 are for SUMO and NEDD8/Rub1, respectively (Johnson and Blobel, 1997; Lammer *et al*, 1998; Osaka *et al*, 1998). In addition, in the autophagic pathway, Atg3 and Atg10 are both E2 enzymes for Atg8 and Atg12, respectively, but they do not have obvious sequence similarities to known Ubc's, except for a short region encompassing an active Cys residue (Shintani *et al*, 1999; Ichimura *et al*, 2000). Similarly, Ufc1 is a unique E2-like enzyme with no obvious sequence homology with other E2s, except approximately 10 amino-acid residues encompassing the active site Cys residue.

In assessing the biological roles of the Ufm1-modifying system, characterization of the target molecule(s) is of particular importance. Regarding this issue, we identified several putative proteins that are conjugated with Ufm1 in human HEK293 cells and various mouse tissues. It is noteworthy that the sizes of these bands (28, 38, 47 kDa) increase by 10 kDa, which is consistent with the size of Ufm1. Considering that several Ubl modifiers can attach to target proteins as a polymer, it is possible that these bands correspond to multi- or poly-Ufm1 conjugates. In fact, Ufm1 has six Lys residues. Whether Ufm1 is conjugated to several distinct proteins or multiple Lys residues in a single target or polymerized in a single Lys residue awaits future study. Unfortunately, we could not identify the protein, and detailed analysis of the cellular function of Ufm1 conjugation awaits future study. It was recently reported that Uba5 is induced by certain reagents that induce stress in the endoplasmic reticulum (ER), a so-called 'unfolded protein response' (Harding *et al*, 2003). However, we could not observe the induction of Uba5, Ufc1, and Ufm1 by treatment with various compounds known to induce ER stress in mammalian cells (data not shown). In addition, exposure to other stresses including high temperature or heavy metals also did not induce the appearance of obvious new conjugation band(s) of Ufm1, by immunoblot analysis. Further studies on the biological roles of the Ufm1 conjugation pathway are under investigation in our laboratories.

Materials and methods

DNA construction

The cDNA encoding human Uba5 was obtained by PCR from human liver cDNA with the Uba5-s5′ primer (5′-CGGAGGGATCCCCATGGCGGAGTCTGTGGAG-3′) and the Uba5-r3′ primer (5′-CAGTCCTCGAGCTACATATTCTTCATTTT-3′). It was then subcloned into pcDNA3 vector (Invitrogen, San Diego, CA). A point mutation for Cys at position 250 to Ser or Ala was generated by PCR-based site-directed mutagenesis. The Flag tag was introduced at the N-terminus of Uba5 or Uba5^{C250S}. Similarly, cDNA encoding human Ufm1 was amplified by PCR from human liver cDNA with the Ufm1-s5′ primer (5′-TTCCGGGATCCCCATGTCGAAGGTTTCCTTT-3′) and the Ufm1-r3′ primer (5′-AGTAGCTCGAGTTAACAACTTCCAACACGAT-3′), and subcloned into pcDNA3 vector. The Flag, FlagHis, or Myc tags were introduced at the N-terminus of Ufm1. The HA tag was introduced at the C-terminus of Ufm1. The C-terminal deletion mutants of Ufm1 named Ufm1ΔC2 and Ufm1ΔC3, encoding amino acids 1–83 and 1–82, respectively, were generated by PCR. A point mutation for Gly at position 83 to Ala of Ufm1 and Ufm1ΔC2 (Ufm1^{G83A} and Ufm1ΔC2^{G83A}, respectively) was generated by PCR-based site-directed mutagenesis. The cDNA encoding human Ufc1 was obtained by PCR from human liver cDNA with the Ufc1-s5′ primer (5′-GCCCTGGATCCAGATGGCGGATGAAGCCACG-3′) and the Ufc1-r3′ primer (5′-TTCTCGAGTCATTGGTTGCATTTCTCTT-3′). It was then subcloned into pcDNA3 vector. A point mutation for Cys at position 116 to Ser or Ala was generated by PCR-based site-directed mutagenesis. The Flag tag was introduced at the N-terminus of Ufc1 and Ufc1^{C116S}. To express GST-fused Ufm1ΔC2, Ufm1ΔC3, Uba5, Uba5^{C250A}, Ufc1, and Ufc1^{C116A} in *E. coli*, these cDNAs were subcloned into pGEX-6p vector (Amersham Biosciences). All mutations mentioned above were confirmed by DNA sequencing.

Cell culture and transfection

Media and reagents for cell culture were purchased from Life Technologies (Grand Island, NY). HEK293 cells were grown in Dulbecco's modified Eagle's medium (DMEM) containing 10% fetal calf serum (FCS), 5 U/ml penicillin, and 50 μg/ml streptomycin. HEK293 cells at subconfluence were transfected with the indicated plasmids using Fugene 6 reagent (Roche Molecular Biochemicals, Mannheim, Germany). Cells were analyzed at 20–24 h after transfection.

Immunological analysis

For immunoblot analysis, cells were lysed with ice-cold TNE buffer (10 mM Tris–HCl, pH 7.5, 1% Nonidet P-40, 150 mM NaCl, 1 mM ethylenediaminetetraacetic acid (EDTA), and protease inhibitors) and the lysates were separated by SDS–PAGE (12% gel or 4–12% gradient gel) and transferred to a polyvinylidene difluoride (PVDF) membrane. Mouse monoclonal anti-Flag antibody (M2; Sigma Chemical Co., St Louis, MO), anti-HA antibody (F7; Santa Cruz Biotechnology, Santa Cruz, CA), and rabbit polyclonal anti-Myc antibody (N14; Santa Cruz) were used for immunodetection. Development was performed by the Western lighting detection methods.

For immunoprecipitation analysis, cells were lysed by 200 μl of TNE, and the lysate was then centrifuged at 10 000 *g* for 10 min at 4°C to remove debris. In the next step, 800 μl of TNE and 30 μl of M2-agarose (Sigma) were added to the lysate, and the mixture was mixed under constant rotation for 12 h at 4°C. The immunoprecipitates were washed five times with ice-cold TNE. The complex was boiled for 10 min in SDS sample buffer in the presence of β-mercaptoethanol to elute proteins and centrifuged at 10 000 *g* for 10 min at 4°C. The supernatant was subjected to SDS–PAGE, transferred to PVDF membrane, and analyzed by immunoblots with anti-Flag (M2) or anti-Myc (N14) antibody.

For purification of 6xHis-tagged proteins under denaturing conditions, cells were lysed by 1 ml of denaturing lysis buffer (8 M urea, 0.1 M NaH_2PO_4, and 0.01 M Tris–HCl, pH 8.0) in the presence of 20 mM *N*-ethylmaleimide as an inhibitor of isopeptidases, and the lysate was sonicated briefly and then centrifuged at 10 000 *g* for 10 min at room temperature to remove debris. Then, 30 μl of Ni-NTA Superflow (QIAGEN) was added to the lysate, and the mixture was shaken under constant rotation for 30 min at room temperature. The precipitates were washed five times with denaturing wash buffer (8 M urea, 0.1 M NaH_2PO_4, and 0.01 M Tris–HCl, pH 5.9). To elute proteins, elution buffer (8 M urea, 0.1 M NaH_2PO_4, and 0.01 M Tris–HCl, pH 4.5) was added to the complex, and the mixture was centrifuged at 10 000 *g* for 10 min at room temperature. The resulting supernatant was subjected to SDS–PAGE, transferred to PVDF membrane, and analyzed by immunoblots with anti-Flag (M2).

Freshly isolated tissues from mice were homogenized in lysis buffer (50 mM Tris–HCl, pH 7.5, 1% SDS, 5 mM EDTA, and 10 mM β-mercaptoethanol) using potter-Elvehjem homogenizer. The homogenate was centrifuged at 10 000 *g* for 10 min to remove debris. The resulting supernatant was subjected to SDS–PAGE, transferred to PVDF membrane, and analyzed by immunoblotting with anti-Ufm1 or preimmune serum. The anti-Ufm1 polyclonal antibody was raised in rabbits using the recombinant protein produced in *E. coli* as an antigen.

In vitro thioester formation assay

Recombinant GST-Ufm1ΔC2, GST-Ufm1ΔC3, GST-Uba5, GST-Uba5^{C250A}, GST-Ufc1, and GST-Ufc1^{C116A} (tagged N-terminally with GST) were produced in *E. coli* and recombinant proteins were purified by chromatography on glutathione sepharose 4B (Amersham Biosciences). After elution of proteins from the beads, the preparations were dialyzed against 50 mM BisTris (pH 6.5), 100 mM NaCl, 10 mM $MgCl_2$, and 0.1 mM DTT (reaction buffer). Most thioester formation reactions contained reaction buffer with 4 μg GST-Ufm1ΔC2 or GST-Ufm1ΔC3 and some of the following: 5 mM ATP, 2 or 0.2 μg GST-Uba5 or GST-Uba5^{C250A}, and 4 μg GST-Ufc1 or GST-Ufc1^{C116A}. Reactions were incubated for 30 min at 25°C and stopped by the addition of SDS-containing loading buffer either lacking reducing agent or containing 100 mM DTT, followed by a 10 min incubation at 37°C, SDS–PAGE (4–12% acrylamide gradient) and Coomassie brilliant blue staining.

Protein identification by LC–MS/MS analysis

The Uba5-associated complexes were digested with *Achromobacter* protease I and the resulting peptides were analyzed using a nanoscale LC–MS/MS system as described previously (Natsume *et al*, 2002). The peptide mixture was applied to a Mightysil-PR-18 (1 μm particle, Kanto Chemical) frit-less column (45 mm × 0.150 mm ID) and separated using a 0–40% gradient of acetonitrile containing 0.1% formic acid over 30 min at a flow rate of 50 nl/min. Eluted peptides were sprayed directly into a quadropole time-of-flight hybrid mass spectrometer (Q-Tof *Ultima*, Micromass, Manchester, UK). MS and MS/MS spectra were obtained in a data-dependent mode. Up to four precursor ions above an intensity threshold of 10 counts/s were selected for MS/MS analyses from each survey scan. All MS/MS spectra were searched against protein sequences of Swiss Prot and RefSeq (NCBI) using batch processes of Mascot software package (Matrix Science, London, UK). The criteria for match acceptance were the following: (1) When the match score was 10 over each threshold, identification was accepted without further consideration. (2) When the difference of score and threshold was lower than 10, or when proteins were identified based on a single matched MS/MS spectrum, we manually confirmed the raw data prior to acceptance. (3) Peptides assigned by less than three y series ions and peptides with +4 charge state were all eliminated regardless of their scores.

Immunofluorescence

HeLa cells grown on glass coverslips were fixed in 4% paraformaldehyde (PFA) in PBS for 15 min, and permeabilized with 0.2% (vol/vol) Triton X-100 in PBS for 30 min. After permeabilization, the cells were blocked for 30 min with 5% (vol/vol) normal goat serum in PBS, incubated for 1 h at 37°C with anti-Ufm1 serum or preimmune serum, washed with PBS, and incubated for 30 min with Alexa 488 nm anti-rabbit antibodies (Molecular Probes). The coverslips were washed and mounted on slides. Fluorescence images were obtained using a fluorescence microscope (DMIRE2; Leica) equipped with a cooled charge-coupled device camera (CTR MIC; Leica). Pictures were taken using Leica Qfluoro software (Leica).

Acknowledgements

We thank T Mizushima (Nagoya University) for the computer-assisted structural modeling of human Ufm1. This work was supported in part by Grants-in-Aid from the Ministry of Education, Culture, Sports, Science and Technology of Japan.

References

Bonifacino JS, Weissman AM (1998) Ubiquitin and the control of protein fate in the secretory and endocytic pathways. *Annu Rev Cell Dev Biol* **14:** 19–57

Cort JR, Chiang Y, Zheng D, Montelione GT, Kennedy MA (2002) NMR structure of conserved eukaryotic protein ZK652.3 from *C. elegans*: a ubiquitin-like fold. *Proteins* **48:** 733–736

D'Cunha J, Knight Jr E, Haas AL, Truitt RL, Borden EC (1996) Immunoregulatory properties of ISG15, an interferon-induced cytokine. *Proc Natl Acad Sci USA* **93:** 211–215

Furukawa K, Mizushima N, Noda T, Ohsumi Y (2000) A protein conjugation system in yeast with homology to biosynthetic enzyme reaction of prokaryotes. *J Biol Chem* **275:** 7462–7465

Glickman MH, Ciechanover A (2002) The ubiquitin-proteasome proteolytic pathway: destruction for the sake of construction. *Physiol Rev* **82:** 373–428

Harding HP, Zhang Y, Zeng H, Novoa I, Lu PD, Calfon M, Sadri N, Yun C, Popko B, Paules R, Stojdl DF, Bell JC, Hettmann T, Leiden JM, Ron D (2003) An integrated stress response regulates amino

acid metabolism and resistance to oxidative stress. *Mol Cell* **11:** 619–633

Hershko A, Ciechanover A (1998) The ubiquitin system. *Annu Rev Biochem* **67:** 425–479

Hodgins RR, Ellison KS, Ellison MJ (1992) Expression of a ubiquitin derivative that conjugates to protein irreversibly produces phenotypes consistent with a ubiquitin deficiency. *J Biol Chem* **267:** 8807–8812

Ichimura Y, Kirisako T, Takao T, Satomi Y, Shimonishi Y, Ishihara N, Mizushima N, Tanida I, Kominami E, Ohsumi M, Noda T, Ohsumi Y (2000) A ubiquitin-like system mediates protein lipidation. *Nature* **408:** 488–492

Jentsch S, Pyrowolakis G (2000) Ubiquitin and its kin: how close are the family ties? *Trends Cell Biol* **10:** 335–342

Johnson ES, Blobel G (1997) Ubc9p is the conjugating enzyme for the ubiquitin-like protein Smt3p. *J Biol Chem* **272:** 26799–26802

Johnson ES, Schwienhorst I, Dohmen RJ, Blobel G (1997) The ubiquitin-like protein Smt3p is activated for conjugation to other proteins by an Aos1p/Uba2p heterodimer. *EMBO J* **16:** 5509–5519

Kabeya Y, Mizushima N, Ueno T, Yamamoto A, Kirisako T, Noda T, Kominami E, Ohsumi Y, Yoshimori T (2000) LC3, a mammalian homologue of yeast Apg8p, is localized in autophagosome membranes after processing. *EMBO J* **19:** 5720–5728

Kamitani T, Nguyen HP, Yeh ET (1997) Preferential modification of nuclear proteins by a novel ubiquitin-like molecule. *J Biol Chem* **272:** 14001–14004

Klionsky DJ, Cregg JM, Dunn Jr WA, Emr SD, Sakai Y, Sandoval IV, Sibirny A, Subramani S, Thumm M, Veenhuis M, Ohsumi Y (2003) A unified nomenclature for yeast autophagy-related genes. *Dev Cell* **5:** 539–545

Klionsky DJ, Emr SD (2000) Autophagy as a regulated pathway of cellular degradation. *Science* **290:** 1717–1721

Komatsu M, Tanida I, Ueno T, Ohsumi M, Ohsumi Y, Kominami E (2001) The C-terminal region of an Apg7p/Cvt2p is required for homodimerization and is essential for its E1 activity and E1–E2 complex formation. *J Biol Chem* **276:** 9846–9854

Lammer D, Mathias N, Laplaza JM, Jiang W, Liu Y, Callis J, Goebl M, Estelle M (1998) Modification of yeast Cdc53p by the ubiquitin-related protein rub1p affects function of the SCFCdc4 complex. *Genes Dev* **12:** 914–926

Liakopoulos D, Doenges G, Matuschewski K, Jentsch S (1998) A novel protein modification pathway related to the ubiquitin system. *EMBO J* **17:** 2208–2214

Liu YC, Pan J, Zhang C, Fan W, Collinge M, Bender JR, Weissman SM (1999) A MHC-encoded ubiquitin-like protein (FAT10) binds noncovalently to the spindle assembly checkpoint protein MAD2. *Proc Natl Acad Sci USA* **96:** 4313–4318

Mizushima N, Noda T, Yoshimori T, Tanaka Y, Ishii T, George MD, Klionsky DJ, Ohsumi M, Ohsumi Y (1998) A protein conjugation system essential for autophagy. *Nature* **395:** 395–398

Nakamura M, Xavier RM, Tsunematsu T, Tanigawa Y (1995) Molecular cloning and characterization of a cDNA encoding monoclonal nonspecific suppressor factor. *Proc Natl Acad Sci USA* **92:** 3463–3467

Natsume T, Yamauchi Y, Nakayama H, Shinkawa T, Yanagida M, Takahashi N, Isobe T (2002) A direct nanoflow liquid chromatography–tandem mass spectrometry system for interaction proteomics. *Anal Chem* **74:** 4725–4733

Ohsumi Y (2001) Molecular dissection of autophagy: two ubiquitin-like systems. *Nat Rev Mol Cell Biol* **2:** 211–216

Osaka F, Kawasaki H, Aida N, Saeki M, Chiba T, Kawashima S, Tanaka K, Kato S (1998) A new NEDD8-ligating system for cullin-4A. *Genes Dev* **12:** 2263–2268

Pickart CM (2001) Mechanisms underlying ubiquitination. *Annu Rev Biochem* **70:** 503–533

Schwartz DC, Hochstrasser M (2003) A superfamily of protein tags: ubiquitin, SUMO and related modifiers. *Trends Biochem Sci* **28:** 321–328

Shintani T, Mizushima N, Ogawa Y, Matsuura A, Noda T, Ohsumi Y (1999) Apg10p, a novel protein-conjugating enzyme essential for autophagy in yeast. *EMBO J* **18:** 5234–5241

Tanaka K, Suzuki T, Chiba T (1998) The ligation systems for ubiquitin and ubiquitin-like proteins. *Mol Cells* **8:** 503–512

Tanida I, Komatsu M, Ueno T, Kominami E (2003) GATE-16 and GABARAP are authentic modifiers mediated by Apg7 and Apg3. *Biochem Biophys Res Commun* **300:** 637–644

Tanida I, Mizushima N, Kiyooka M, Ohsumi M, Ueno T, Ohsumi Y, Kominami E (1999) Apg7p/Cvt2p: a novel protein-activating enzyme essential for autophagy. *Mol Biol Cell* **10:** 1367–1379

Varshavsky A (1997) The ubiquitin system. *Trends Biochem Sci* **22:** 383–387

Walden H, Podgorski MS, Huang DT, Miller DW, Howard RJ, Minor Jr DL, Holton JM, Schulman BA (2003a) The structure of the APPBP1–UBA3–NEDD8–ATP complex reveals the basis for selective ubiquitin-like protein activation by an E1. *Mol Cell* **12:** 1427–1437

Walden H, Podgorski MS, Schulman BA (2003b) Insights into the ubiquitin transfer cascade from the structure of the activating enzyme for NEDD8. *Nature* **422:** 330–334

Yeh ET, Gong L, Kamitani T (2000) Ubiquitin-like proteins: new wines in new bottles. *Gene* **248:** 1–14

Pael-R Is Accumulated in Lewy Bodies of Parkinson's Disease

Tetsuro Murakami, MD, PhD,[1] Mikio Shoji, MD, PhD,[1]
Yuzuru Imai, PhD,[2] Haruhisa Inoue, MD, PhD,[2]
Takeshi Kawarabayashi, MD, PhD,[1]
Etsuro Matsubara, MD, PhD,[1]
Yasuo Harigaya, MD, PhD,[3] Atsushi Sasaki, MD, PhD,[4]
Ryosuke Takahashi, MD, PhD,[2] and Koji Abe, MD, PhD[1]

We examined the distribution of Pael-R, a newly identified substrate for Parkin, in Parkinson's disease (PD) and multiple system atrophy (MSA). Pael-R, Parkin, α-synuclein, and ubiquitin accumulated in Lewy bodies (LBs) and neurites. Pael-R was localized in the core of LBs. Parkin and α-synuclein accumulated in the halo, neuronal cell bodies, and processes. These findings potentially suggest the involvement of Pael-R in LB formation, and protection role of Parkin in Pael-R-mediated neurotoxicity in PD. The absence of Pael-R and Parkin in glial cytoplasmic inclusions (GCIs) in MSA implies a distinct pathway involved in the formation of LBs and GCIs.

Ann Neurol 2004;55:439–442

Parkinson's disease (PD) is the second most frequent neurodegenerative disorder after Alzheimer's disease. Loss of pigmented neurons, gliosis, and the appearance of Lewy bodies (LBs) in the remaining neurons in the substantia nigra are the most common pathological findings.[1] Missense mutations in the α-synuclein gene are cosegregated in a few families with autosomal dominant forms of PD.[2,3] α-Synuclein and its modifications have been identified as the major components of LBs.[4–6] Parkin is another gene responsible for autosomal recessive forms of juvenile PD (AR-JP).[7] Parkin carries a ubiquitin-protein ligase (E3) activity of glycosylated α-synuclein.[5,7] AR-JP–linked deletions of the Parkin gene are defective in this activity.[8] Although no LBs are observed in AR-JP, Parkin is considered to play an important role in LB formation.[9] Yeast two-hybrid screening identified Pael-R (Parkin-associated endothelin receptor–like receptor) as another substrate for Parkin.[10,11] Newly synthesized Pael-R is folded into the endoplasmic reticulum (ER) and then transported to the cell membrane. Misfolded Pael-R is normally translocated across the ER membrane into the cytosol and degradated through the ubiquitin-proteasome pathway. However, excessive amounts of unfolded Pael-R in the ER cause unbearable stress and decrease cell viability, which finally leads to cell death in cultured cells.[11] Parkin inhibits ER stress–mediated cell death by ubiquitinating Pael-R and promoting degradation of misfolded and aggregated Pael-R.[11,12] Therefore, there is a possibility that these molecules participate in the pathological pathway initiating from the formation of LBs in PD and dementia with Lewy bodies (DLB). To elucidate this hypothesis, we examined the midbrains of patients with PD or DLB and compared them with those of normal controls and those with multiple system atrophy (MSA), another neurodegenerative disorder showing a pathological lesion composed of aggregates of insoluble α-synuclein as glial cytoplasmic inclusions (GCIs).[13]

Materials and Methods

A total of 21 autopsy brains from six patients with PD (aged 64–81 years), three with DLB (aged 73–84 years), six with MSA (aged 51–66 years), and six normal controls (aged 45–91 years) were enrolled. Polyclonal anti–Pael-R (diluted 1:5) and anti-Parkin (diluted 1:20) antibodies were raised in rabbits against C-terminal 62 amino acids of human Pael-R expressed in bacteria and FLAG-Parkin protein expressed in 293 cells, respectively. Details of the antibodies have been described elsewhere.[11,12] LB509, a monoclonal antibody for α-synuclein (diluted 1:20),[4] and a rabbit polyclonal antibody for ubiquitin (Ubi-Q, diluted 1:1,000) also were used. Paraffin-embedded midbrain sections were pretreated with 99% formic acid for 3 minutes before staining with antibodies for Parkin, α-synuclein and ubiquitin. Sections were blocked with 10% normal goat or horse serum, incubated with primary antibodies overnight at room temperature, immunostained using an ABC immunostaining kit (Vector, Burlingame, CA), and then stained by hematoxylin nuclear staining.

Results

Anti–Pael-R antibody labeled LBs in the midbrains of all the PD patients. Approximately 90% of the LBs detected by LB509 staining were labeled by the antibody. Pael-R was localized more intensely in the core

From the [1]Department of Neurology, Okayama University Graduate School of Medicine and Dentistry, Okayama; [2]Laboratory for Motor System Neurodegeneration, RIKEN Brain Science Institute, Saitama; [3]Department of Neurology, Maebashi Red Cross Hospital; and [4]First Department of Pathology, Gunma University School of Medicine, Gunma, Japan.

Received Oct 10, 2003, and in revised form Jan 3, 2004. Accepted for publication Jan 5, 2004.

Address correspondence to Dr Shoji, Department of Neurology, Okayama University Graduate School of Medicine and Dentistry, 2-5-1 Shikata-cho, Okayama 700-8558, Japan.
E-mail: mshoji@cc.okayama-u.ac.jp

Published by Wiley-Liss, Inc., through Wiley Subscription Services

of most LBs (Fig 1A, B) and in the halo of some LBs (see Fig 1C), whereas neuronal cytoplasm was not stained. The same immunoreactivity of LBs was observed in all DLB patients. A substantial part of Lewy neurites was also positive for the antibody (see Fig 1D). Anti–Parkin antibody labeled LBs in all the PD patients. The appearance rate of immunoreactive LBs was the same as that stained with anti–Pael-R antibody. The halo was labeled more intensely (see Fig 1F–H), and the cytoplasm and proximal processes of the neurons were stained intensely in a punctuated pattern. Substantial Lewy neurites also were stained (see Fig 1I). There was no difference in the immunoreactivities between the PD and DLB patients. LB509 labeled almost all LBs in the midbrains, especially the halo, of all the PD patients (see Fig 1K–M). α-Synuclein accumulated as small granules in the cytoplasm of many neurons (see Fig 1M) and neurites (see Fig 1N). The same immunohistological findings were observed in DLB patients. Distributions of LBs and Lewy neurites in the midbrains stained with antibodies for α-synuclein, Pael-R, and Parkin corresponded. Ubi-Q labeled LBs, cytoplasm, and Lewy neurites in the PD and DLB patients. Although most LBs were labeled intensely in the halo (see Fig 1P, Q, arrow), some LBs were stained more strongly in the core (see Fig 1Q, arrowheads, R). Lewy neurites were also positive for Ubi-Q (see Fig 1S). Ubiquitin-positive LBs composed approximately 90% of those detected with LB509 staining. In the normal controls, no neurons or LBs were labeled by antibodies for Parkin, Pael-R, α-synuclein, or ubiquitin in the substantia nigra (see Fig 1E, J, O, and T).

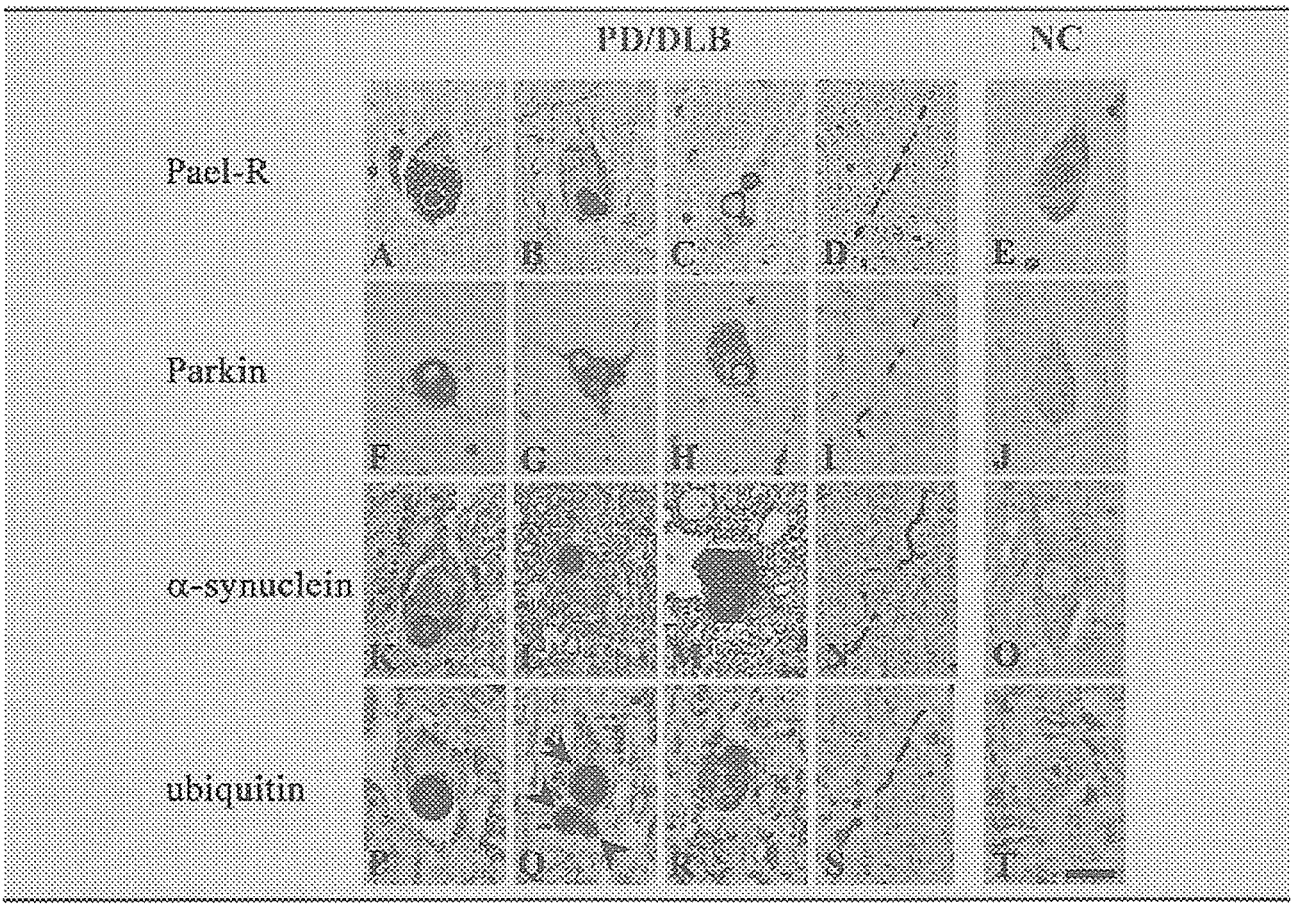

Fig 1. Immunostaining of Lewy bodies or Lewy neurites and normal controls with anti–Pael-R antibody (A–E), anti–Parkin antibody (F–J), LB509 (K–O), and Ubi-Q (P–T) in Parkinson's disease (PD). Polyclonal rabbit antibodies were affinity purified. LBs showed intense staining of Pael-R in the core (A, B) and in some peripheral halos (C). Pael-R also was localized to Lewy neurites (D). Parkin was prominently accumulated in the halo, cytoplasm (F–H), and Lewy neurites (I) of the PD or dementia with Lewy bodies (DLBs) brains. α-Synuclein was present mainly in the halo of LBs (K, L), but also in the neuronal cytoplasm (M) and Lewy neurites (N) in the substantia nigra. Ubiquitin was present in peripheral halos (P and Q, arrow*), in LB cores (Q,* arrowheads*, R), and in Lewy neurites (S). B, C, and H are from DLB brains, and the others are from PD brains. For a preabsorption study, the antibody solution, including 10μg/ml Pael-R protein and 2% bovine serum albumin, was preincubated and centrifuged at 36,000 rpm before staining. A preabsorption test for Pael-R antibody did not show any signals. NC = normal control. Scale bar = 50μm.*

In the crus cerebri of the MSA patients, no GCIs were labeled by anti–Pael-R antibody (Fig 2A) or anti–Parkin antibody (see Fig 2B). However, immunostaining with LB509 (see Fig 2C) and Ubi-Q (see Fig 2D) demonstrated extensive distributions of immunoreactive GCIs. The cytoplasm of oligodendrocytes was labeled diffusely by LB509 and Ubi-Q. No neuronal accumulation of Pael-R, Parkin, α-synuclein, or ubiquitin was observed in the MSA patients.

Discussion

Because no immunoreactivities of Pael-R, Parkin, α-synuclein, or ubiquitin were observed in the neurons of normal controls and MSA patients, the accumulation of these molecules in the midbrains of the PD and DLB patients is strongly suggested. Although paraffin-embedded sections show a decrease in the immunoreactivity of normally expressed proteins, they are still useful for the histological detection of accumulated proteins. Enhanced staining by formic acid pretreatment supports these findings. A previous report showed a substantial expression of Parkin in the neurons of normal controls.[9] However, our immunostaining was negative at normal expression levels. Thus, the molecules involved in the ubiquitin-proteasome pathway, Pael-R, Parkin, α-synuclein, and ubiquitin, accumulate in neurons and are closely related to LBs and Lewy neurites in PD and DLB patients.

In this study, Pael-R was localized prominently in the core of LBs and Lewy neurites, whereas Parkin and α-synuclein were observed in the halo, as well as neuronal cell bodies and processes. The distribution of Pael-R resembled that of ubiquitin. The different distributions of these molecules may suggest distinct roles in LB formation. LBs consist of dense vesicles in the core and radiating filaments in the halo in electron microscopy,[14] suggesting that aggregated proteins form filaments in the core of LBs. These findings indicate that aggregated Pael-R is a major component of LBs, and that Parkin in the core of LBs may not be effective in degrading aggregated Pael-R in the ubiquitin-proteasome pathway.

To date, several candidates have been identified as substrates of Parkin and shown to be present in LBs: α-synuclein,[5] synphilin-1,[15] p38,[16] and synaptotagmin X1.[17] We showed that Pael-R is a novel substrate of Parkin that accumulates in the LBs of PD and DLB patients. Because unfolded and insoluble aggregates of Pael-R cause ER stress–mediated cell death in cultured cell models, our findings indicate the presence of a pathway from the initial accumulation of Pael-R to the formation of LBs, and finally to dopaminergic neuronal cell loss in PD and DLB brains. The substrates of Parkin share a common feature: they easily become misfolded and aggregated.[5,11] Parkin promotes the ubiquitination and degradation of the misfolded proteins.[11,12] Recent reports have identified a failure in the ubiquitin-proteasome pathway in PD,[18] which might be a pathogenic factor underlying the accumulation and inclusion formation of misfolded proteins such as Pael-R. The presence of Parkin and ubiquitin in LBs also supports this hypothesis.

We showed that Pael-R and Parkin did not accumulate in GCIs, whereas α-synuclein and ubiquitin were localized in both LBs and GCIs. Recent studies have shown several proteins, including α-synuclein and synphilin-1, as common components of LBs and GCIs.[13,19] Localization of α-synuclein in LBs and

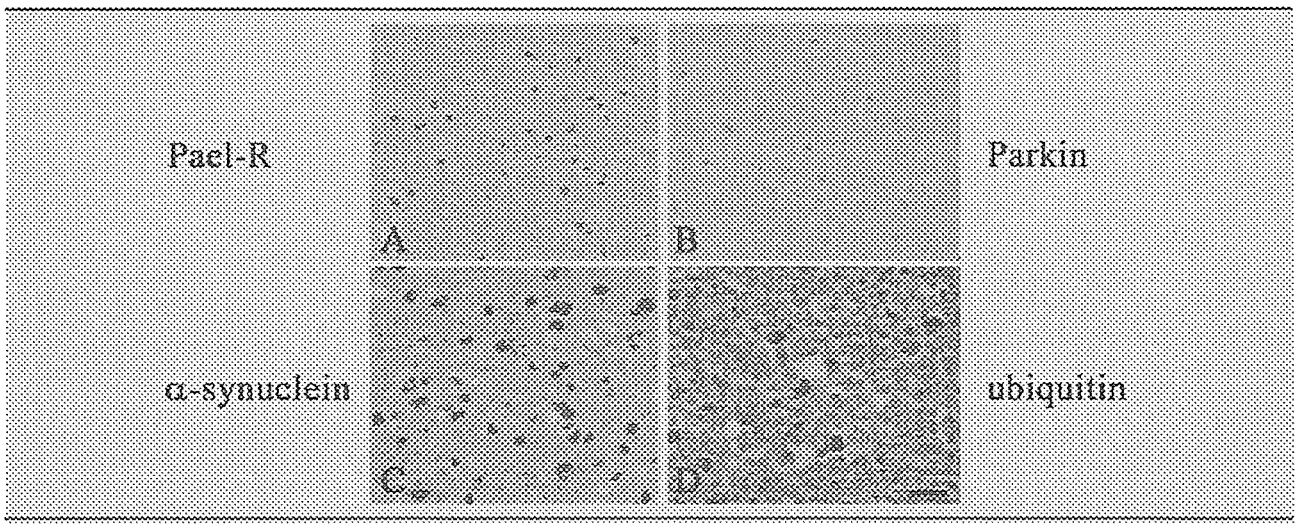

Fig 2. Immunostaining of glial cytoplasmic inclusions (GCIs) in multiple system atrophy (MSA) patients with anti–Pael-R antibody (A), anti–Parkin antibody (B), LB509 (C), and Ubi-Q (D). Pael-R and Parkin were not accumulated in GCIs (A, B, respectively), but many α-synuclein- and ubiquitin-positive GCIs were present in the crus cerebri (C, D, respectively). Scale bar = 50μm.

GCIs implies that a common mechanism, such as α-synucleinopathy, is underlying among PD, DLB, and MSA. However, the absence of Pael-R and Parkin in GCIs indicates a distinct rather than common mechanism in the formation of intracellular inclusions consisting of α-synuclein. Parkin and Pael-R may play a unique role in LB formation and not just any inclusions such as GCIs. Prominent neuronal expression of Pael-R and Parkin in the human brain also may explain the distinct finding of LBs.[11,20] Further study of the roles of Pael-R and Parkin, especially their involvement with LBs, will be of great help in understanding the pathogenesis of PD.

This study was supported by Grants-in-Aid from the Primary Amyloidosis Research Committee , surveys and research on special diseases from the Ministry of Health, Labor and Welfare of Japan and by Grants-in-Aid for Scientific Research (B) (14370208) and Scientific Research on Priority Areas (C)–Advanced Brain Science Project from the Ministry of Education, Culture, Sports, Science and Technology, Japan.

Antibody LB509 and Ubi-Q were kind gifts from T. Iwatsubo and D.W. Dickson, respectively.

References

1. Lotharius J, Brundin P. Pathogenesis of Parkinson's disease: dopamine, vesicles and alpha-synuclein. Nat Rev Neurosci 2002; 3:932–942.
2. Polymeropoulos MH, Lavedan C, Leroy E, et al. Mutation in the α-synuclein gene identified in families with Parkinson's disease. Science 1997;276:2045–2047.
3. Krüger R, Kuhn W, Müller T, et al. Ala30Pro mutation in the gene encoding α-synuclein in Parkinson's disease. Nat Genet 1998;18:106–108.
4. Baba M, Nakajo S, Tu PH, et al. Aggregation of α-synuclein in Lewy bodies of sporadic Parkinson's disease and dementia with Lewy bodies. Am J Pathol 1998;152:879–884.
5. Shimura H, Schlossmacher MG, Hattori N, et al. Ubiquitination of a new form of alpha-synuclein by parkin from human brain: implications for Parkinson's disease. Science 2001;293: 263–269.
6. Fujiwara H, Hasegawa M, Dohmae N, et al. α-Synuclein is phosphorylated in synucleinopathy lesions. Nat Cell Biol 2002; 4:160–164.
7. Kitada T, Asakawa S, Hattori N, et al. Mutations in the parkin gene cause autosomal recessive juvenile parkinsonism. Nature 1998;392:605–608.
8. Shimura H, Hattori N, Kubo S, et al. Familial Parkinson disease gene product, parkin, is a ubiquitin-protein ligase. Nat Genet 2000;25:302–305.
9. Schlossmacher MG, Frosch MP, Gai WP, et al. Parkin localizes to the Lewy bodies of Parkinson disease and dementia with Lewy bodies. Am J Pathol 2002;160:1655–1667.
10. Zeng Z, Su K, Kyaw H, Li Y. A novel endothelin receptor type-B-like gene enriched in the brain. Biochem Biophys Res Commun 1997;233:559–567.
11. Imai Y, Soda M, Inoue H, et al. An unfolded putative transmembrane polypeptide, which can lead to endoplasmic reticulum stress, is a substrate of Parkin. Cell 2001;29:891–902.
12. Imai Y, Soda M, Takahashi R. Parkin suppresses unfolded protein stress-induced cell death through its E3 ubiquitin-protein ligase activity. J Biol Chem 2000;275:35661–35664.
13. Shoji M, Harigaya Y, Sasaki A, et al. Accumulation of NACP/α-synuclein in Lewy body disease and multiple system atrophy. J Neurol Neurosurg Psychiatry 2000;68:605–608.
14. Forno LS. Neuropathology of Parkinson's disease. J Neuropathol Exp Neurol 1996;55:259–272.
15. Chung KK, Zhang Y, Lim KL, et al. Parkin ubiquitinates the α-synuclein-interacting protein, synphilin-1: implications for Lewy-body formation in Parkinson disease. Nat Med 2001;7: 1144–1150.
16. Corti O, Hampe C, Koutnikova H, et al. The p38 subunit of the aminoacyl-tRNA synthetase complex is a Parkin substrate: linking protein biosynthesis and neurodegeneration. Hum Mol Genet 2003;12:1427–1437.
17. Huynh DP, Scoles DR, Nguyen D, Pulst SM. The autosomal recessive juvenile Parkinson disease gene product, parkin, interacts with and ubiquitinates synaptotagmin XI. Hum Mol Genet 2003;12:2587–2597.
18. McNaught KS, Olanow CW, Halliwell B, et al. Failure of the ubiquitin-proteasome system in Parkinson's disease. Nat Rev Neurosci 2001;2:589–594.
19. Wakabayashi K, Engelender S, Tanaka Y, et al. Immunocytochemical localization of synphilin-1, an alpha-synuclein-associated protein, in neurodegenerative disorders. Acta Neuropathol 2002;103:209–214.
20. Solano SM, Miller DW, Augood SJ, et al. Expression of α-synuclein, parkin, and ubiquitin carboxy-terminal hydrolase L1 mRNA in human brain: genes associated with familial Parkinson's disease. Ann Neurol 2000;47:201–210.

Journal of Neurochemistry, 2004, **90**, 231–244 doi:10.1111/j.1471-4159.2004.02486.x

CHIP promotes proteasomal degradation of familial ALS-linked mutant SOD1 by ubiquitinating Hsp/Hsc70

Makoto Urushitani,*[,1] Junko Kurisu,* Minako Tateno,* Shigetsugu Hatakeyama,† Kei-Ichi Nakayama,† Shinsuke Kato‡ and Ryosuke Takahashi*

*Laboratory for Motor System Neurodegeneration, RIKEN Brain Science Institute, Wako, Saitama, Japan

†Division of Cell Biology, Department of Molecular and Cellular Biology, Medical Institute of Bioregulation, Kyushu University, Fukuoka, Japan

‡Department of Neuropathology, Institute of Neurological Science, Faculty of Medicine, Tottori University, Tottori, Japan

Summary

Over 100 mutants in superoxide dismutase 1 (SOD1) are reported in familial amyotrophic lateral sclerosis (ALS). However, the precise mechanism by which they are degraded through a ubiquitin-proteasomal pathway (UPP) remains unclear. Here, we report that heat-shock protein (Hsp) or heat-shock cognate (Hsc)70, and the carboxyl terminus of the Hsc70-interacting protein (CHIP), are involved in proteasomal degradation of mutant SOD1. Only mutant SOD1 interacted with Hsp/Hsc70 *in vivo*, and *in vitro* experiments revealed that Hsp/Hsc70 preferentially interacted with apo-SOD1 or dithiothreitol (DTT)-treated holo-SOD1, compared with metallated or oxidized forms. CHIP, a binding partner of Hsp/Hsc70, interacted only with mutant SOD1 and promoted its degradation. Both Hsp70 and CHIP promoted polyubiquitination of mutant SOD1-associated molecules, but not of mutant SOD1, indicating that mutant SOD1 is not a substrate of CHIP. Moreover, mutant SOD1-associated Hsp/Hsc70, a known substrate of CHIP, was polyubiquitinated *in vivo*, and polyubiquitinated Hsc70 by CHIP interacted with the S5a subunit of the 26S proteasome *in vitro*. Furthermore, CHIP was predominantly expressed in spinal neurons, and ubiquitinated inclusions in the spinal motor neurons of $hSOD1^{G93A}$ transgenic mice were CHIP-immunoreactive. Taken together, we propose a novel pathway in which ubiquitinated Hsp/Hsc70 might deliver mutant SOD1 to, and facilitate its degradation, at the proteasome.

Keywords: amytrophic lateral sclerosis, CHIP, Hsp70, proteasome degradation, superoxide dismutase 1, ubiquitin.

J. Neurochem. (2004) **90,** 231–244.

Amyotrophic lateral sclerosis (ALS) is a fatal neurodegenerative disease characterized by progressive palsy in limbs and bulbar muscles. A genetic mutation in superoxide dismutase 1 (SOD1) was identified in 1993 as a causal defect shared in 20% of familial ALS patients (Rosen *et al.* 1993). Although SOD1 is an antioxidant enzyme, accumulating lines of evidence strongly support a 'gain of toxic function hypothesis' rather than a 'loss of function hypothesis' (Cleveland and Rothstein 2001; Julien 2001).

Recent lines of evidence indicate that the misfolded nature of mutant SOD1 is a distinct feature common in over 100 mutants (Valentine and Hart 2003). Several misfolded forms taken by mutant SOD1 reportedly include a non-native oligomer, a soluble aggregate, and a detergent-insoluble aggregate (Johnston *et al.* 2000; Shinder *et al.* 2001; Urushitani *et al.* 2002). In addition, most types of mutant SOD1 are more readily monomerized by a reducing agent

Received October 6, 2003; revised manuscript received January 23, 2004; accepted March 3, 2004.

Address correspondence and reprint requests to Ryosuke Takahashi, MD, PhD, Laboratory for Motor System Neurodegeneration, RIKEN Brain Science Institute, 2–1 Hirosawa, Wako, Saitama 351–0198, Japan. E-mail: ryosuke@brain.riken.go.jp

[1]The present address of Makoto Urushitani is Department of Molecular Endocrinology, Research Centre of the CHUL (Centre Hospitalier de l'Université Laval), 2705 boul. Laurier, Québec, Canada, G1V4G2.

Abbreviations used: ALS, amyotrophic lateral sclerosis; CHIP, carboxyl terminus of Hsc70-interacting protein; CHX, cycloheximide; DTT, dithiothrietol; E1, ubiquitin activating enzyme; E2, ubiquitin converting enzyme; E3, ubiquitin ligase; EIP, immunoprecipitation; GST, glutathione-S-transferase; HA, hemagglutinin; Hsc, heat-shock cognate protein; Hsp, heat-shock protein; IB, immunoblotting; LBHIs, Lewy body-like hyaline inclusions; 2ME, 2-mercaptoethanol; SOD1, superoxide dismutase 1; TPR, tetratricopeptide repeat; UPP, ubiquitin-proteasomal pathway.

than the wild-type, thus allowing their intramolecular hydrophobic amino acid residues to be exposed to cytoplasm (Tiwari and Hayward 2003). Other groups have demonstrated that the apo-state enhances the instability of mutant SOD1 (Lindberg *et al.* 2002). These features might be the molecular basis for degradation of mutant SOD1 through the ubiquitin-proteasomal pathway (UPP) (Nakano *et al.* 1996; Johnston *et al.* 2000). We previously demonstrated that mutant, not wild-type, SOD1 is conjugated to a multiubiquitin chain and degraded at the proteasome (Urushitani *et al.* 2002). Although the precise mechanism underlying UPP for handling mutant SOD1 is still an enigma, a mutant SOD1-specific ubiquitin ligase has been proposed (Niwa *et al.* 2002).

However, since over 100 mutants of FALS-related SOD1 have been identified, its recognition mechanism may rely upon a common mediator. In this context, a molecular chaperone, especially heat shock protein 70 (Hsp70), is a very attractive candidate. Overexpression of Hsp70 in cultured motor neurons rescues them from mutant SOD1-induced apoptosis (Bruening *et al.* 1999). This group also reported that detergent-insoluble, but not detergent-soluble, mutant SOD1 associates with Hsp70 in spinal cord lysates from G93A transgenic mice (Shinder *et al.* 2001). Moreover, mutant SOD1 interacts with Hsp70 under heat-shock conditions (Okado-Matsumoto and Fridovich 2002). Pathologically, hSOD1-immunoreactive inclusions in spinal cord of the patients or transgenic mice expressing mutant SOD1 are frequently stained with antibody against heat-shock cognate (Hsc)70, a constitutively expressed form of Hsp70 (Watanabe *et al.* 2001). However, the role of Hsp/Hsc70 in mutant SOD1 metabolism remains unclear. Interestingly, Hsc70 facilitates the degradation of several proteins at the proteasome in a ubiquitination-dependent manner (Bercovich *et al.* 1997), suggesting a role for Hsp/Hsc70 in handling various types of misfolding proteins for proteasomal degradation. For instance, the rate of degradation of androgen receptors containing expanded polyglutamine in bulbospinal muscular atrophy was accelerated by Hsp70 both in cells (Bailey *et al.* 2002) and transgenic mice (Adachi *et al.* 2003).

The carboxyl terminus of Hsc70-interacting protein (CHIP) contains a tetratricopeptide repeat (TPR) domain with which Hsp/Hsc 70 interacts, and inhibits chaperoning by Hsp/Hsc70 through a decrease in ATPase activity (Ballinger *et al.* 1999; Aravind and Koonin 2000). To date, various molecules have been identified as CHIP substrates, including glucocorticoid receptors (Connell *et al.* 2001), misfolded cystic fibrosis transmembrane-conductance regulator (CFTR) (Meacham *et al.* 2001), heat-denatured luciferase (Murata *et al.* 2001) and transmembrane receptor tyrosine kinase ErbB2 (Xu *et al.* 2002). The wild-type androgen receptor containing a normal polyglutamine repeat is also ubiquitinated by CHIP (Cardozo *et al.* 2003).

This study investigated the role of Hsp/Hsc70 and CHIP in the degradation of mutant SOD1 in UPP. Evidence is provided that CHIP promotes the formation of a ubiquitin-mutant SOD1 complex and proteasomal degradation. Surprisingly, however, this effect was not caused by ubiquitination of mutant SOD1, but of Hsp/Hsc70. This result indicates that ubiquitinated Hsp/Hsc70 recruits mutant SOD1 toward the proteasome. This is a novel pathway that explains the degradation mechanism of more than 100 mutant SOD1, as well as the pathology of ALS.

Experimental procedures

Materials

Antisera specific for His-CHIP were prepared in rabbits (Imai *et al.* 2002). Bovine Hsc70 was purchased from Medical and Biological Laboratories (Nagoya, Japan). Purified human E1, ubiquitin converting enzyme (E2; ubcH5a) and ubiquitn aldehyde were purchased from Boston Biochem (Cambridge, MA, USA). Rabbit polyclonal anti-hSOD1 and monoclonal antibody recognizing both Hsc70 and Hsp70 (C92F3 A-5) were purchased from StressGen (Victoria, BC, Canada). Rat monoclonal anti-HA (3F10) antibodies was purchased from Roche (Basel, Switzerland). Mouse monoclonal anti-V5 tag antibody was purchased from Invitrogen (Carlsbad, CA, USA).

Plasmid construction

Human SOD1 cDNA (hSOD1), with or without the FLAG-tag (wild-type, G85R or G93A mutant), was produced as previously described (Urushitani *et al.* 2002). pcDNA3.1-human Hsp70-V5 was a generous gift from N. Nukina (RIKEN Brain Science Institute). The preparation of hemagglutinin (HA)-tagged ubiquitin (HA-Ub) and CHIP cDNAs is described elsewhere (Hatakeyama *et al.* 2001). cDNA construction of mutant CHIP, devoid of tetratricopeptide repeat or U-box (ΔTPR or ΔU-box), was conducted by inverted PCR, using the primer pairs: 5′-ACTCGGGCTC TTATCAGGGCTGCC-3′ and 5′-CAGCGACTCAACTTTGGGGA TGATA-3′ for ΔTPR, and 5′-GTCAGGGATATCTCGCTTCTT TCTT-3′ and 5′-ATTGACGCTTTCATCTCTGAGAACG-3′ for ΔU-box. PCR products were ligated into pcDNA3 containing either the HA or Myc tag sequence at the 5′ end. 6 × His-tagged CHIP recombinant protein was produced by subcloning CHIP cDNA into pET28a(+) vector at the EcoRI/XhoI sites (Novagen, Madison, WI, USA). 6 × His-tagged Hsp70 (His-Hsp70) of full length and deletion mutant of carboxyl terminus (ΔC) or of ATPase domain (ΔATP), was produced as previously reported (Imai *et al.* 2002).

Purification of recombinant proteins

Recombinant glutathione S-transferase-fused hSOD1 (GST-hSOD1) with or without FLAG-tag at the 3′ terminus was generated as previously reported (Kang and Eum 2000; Urushitani *et al.* 2002) with minor modifications. After digestion of GST-hSOD1 ± FLAG to be released from GST, the hSOD1 proteins were demetallated by overnight incubation in 100 mM EDTA, followed by additional overnight incubation in acetate pH 3.8. Finally, they were dialyzed against a buffer containing 50 mM Tris-HCl pH 7.5 and 100 mM

NaCl (Buffer A). Metallation was performed by incubation in two equivalent parts of zinc chloride for 24 h, followed by further incubation with two-equimolar copper chloride for 24 h. The activity of demetallated or remetallated recombinant SOD1 was confirmed using a SOD1 activity assay kit (Dojindo, Kumamoto, Japan), in which dismutase activity against the superoxide anion, generated from the reaction of xanthine with xanthine oxidase, was quantified (data not shown). For several experiments, metallated SOD1 proteins were incubated with hydrogen peroxide for 1 h at room temperature, followed by overnight dialysis against buffer A. Demetallated, metallated or oxidized SOD1 was stored at −80°C until use. Recombinant 6 × His-tagged CHIP (His-CHIP) and HA-tagged ubiquitin were produced as previously reported (Hatakeyama *et al.* 2001; Imai *et al.* 2002).

Cultures and transfection

Murine neuroblastoma cell-line, Neuro2a cells were maintained in Dulbecco's minimum essential medium (DMEM) containing 10% fetal bovine serum (FBS). Transfection was performed using Lipofectamin PLUS (Invitrogen) according to the manufacturer's protocol. The medium was replaced with one containing 5 mM dibutylyl cyclic-AMP (db-cAMP) 3 h after transfection to differentiate cells. Twenty-four hours after transfection, cells were harvested and processed for immunoprecipitation or immunoblotting.

Immunoblotting

Cultured cells were harvested and lysed by the following buffers depending on the experiment: TNG-T buffer consisting of 50 mM Tris-HCl pH 7.4, 150 mM NaCl, 10% glycerol, 1% Triton X-100 and a protease inhibitor cocktail (Roche); RIPA buffer consisting of 20 mM HEPES pH 7.4, 150 mM NaCl, 2 mM EDTA, 1% Nonidet-P40, 1% sodium deoxycholate, 0.1% sodium dodecyl sulfate (SDS) and protease inhibitor cocktail; and denaturing buffer consisting of 20 mM Tris-HCl pH 7.5, 1% SDS, 2 mM EDTA and 1 mM dithiothreitol (DTT). Cells were briefly sonicated on ice in TNG-T buffer or RIPA buffer, or were sonicated and boiled for 5 min at 95°C in the denaturing buffer before centrifugation (10 400 *g* for 30 min). The supernatant fluids were analyzed for immunoprecipitation or western blotting after protein concentration was determined by the Coomassie protein assay kit or bicinchoninic acid (BCA) protein assay kit (Pierce, Rockford, IL, USA). In most experiments, the lysates were denatured using equal amounts of 4% SDS sample buffer containing 2-mercaptoethanol (2ME) for 5 min at 95°C, separated by SDS- polyacrylamide gel electrophoresis (denaturing-PAGE) and transferred to polyvinylidene difluoride (PVDF) membrane (Millipore, Billerica, MA, USA). In several experiments investigating the proportion of dimer and monomer in SOD1 protein, lysates were incubated with equal amounts of 1% SDS sample buffer without 2ME for 15 min at 37°C before SDS-PAGE (partially denaturing PAGE). A western blot image was obtained using an enhanced chemiluminescence detection kit (ECL; Amersham Bioscience, Piscataway, NJ, USA) and quantified using Scion Image software (Scion Corp., Frederick, MD, USA) in several experiments.

Immunoprecipitation and *in vivo* ubiquitination assay

For immunoprecipitation, different cell lysis buffers were used depending on *in vivo* experiments. The TNG-T buffer was used to study the interaction between SOD1 and Hsp/Hsc70. For *in vivo* ubiquitination assay, RIPA buffer was used. Twenty-four hours after transfection of the cells in 6-well culture plates, cell lysates prepared as described previously were incubated with anti-V5 antibody and protein G sepharose to immunoprecipitate Hsp70-V5 (×500 dilution), or anti-FLAG affinity gel (Sigma, St Louis, MO, USA) to immunoprecipitate SOD1-FLAG, for overnight or 1 h at 4°C, respectively. Immunoprecipitates were washed five times in RIPA buffer and eluted in 2% SDS sample buffer by boiling for 5 min at 95°C. In partially denaturing PAGE, immunoprecipitates were eluted in 0.5% SDS sample buffer without 2ME for 15 min at 37°C. The eluate was analyzed by western blotting.

In *in vivo* ubiquitination assay, HA-ubiquitin was expressed in Neuro2a cells in addition to other constructs. After immunoprecipitation as described above, western analysis was carried out using anti-HA antibody as previously reported (Urushitani *et al.* 2002). However, since non-covalent interaction was not completely disrupted by RIPA buffer, it is unclear whether polyubiquitinated species are SOD1. Therefore, when covalently ubiquitinated molecules were examined, cells were solubilized in denaturing buffer containing 1% SDS (see above) with 5 min boiling. Subsequently, the lysate was diluted in a 10-fold volume of dilution buffer (20 mM Tris-HCl pH 7.5, 2 mM EDTA) before immunoprecipitation. Covalent ubiquitination of the target proteins was evaluated using antibodies against HA or the substrate proteins (Jiang *et al.* 2001).

Monomer-dimer transition study of SOD1

SOD1 possesses an unusual intrasubunit disulfide bond to stabilize its dimer formation (Abernethy *et al.* 1974). The holo-state SOD1 dimer contact is tight enough to be resistant to mild SDS denaturation. On the other hand, a reducing agent such as DTT or 2ME is required for complete monomerization in addition to boiling with SDS (Abernethy *et al.* 1974). Remetallated recombinant SOD1-FLAG proteins were treated by H_2O_2 (0.1 or 1 mM) for 1 h at room temperature or by DTT (0.1, 1.0 or 10 mM) for 1 h at 37°C. Proteins were incubated with an equal amount of 1% SDS sample buffer without 2ME for 15 min at 55°C, before SDS-PAGE (partially denaturing PAGE) and western blotting using anti-SOD1 antibody as described above.

In vitro binding assay

We investigated the molecular features of SOD1 protein that interact with Hsc70 by *in vitro* binding study. First, mouse monoclonal anti-Hsp/Hsc70 antibody was incubated overnight with Protein G sepharose (1 μg per 10 μL sepharose) at 4°C. Recombinant SOD1-FLAG proteins (0.4 μM), which were demetallated, remetallated or treated with hydrogen peroxide (0.1 or 1.0 mM) or 1 mM DTT as described above, and bovine Hsc70 (0.2 μM), were mixed in a binding buffer consisting of 50 mM Tris-HCl pH 7.5, 100 mM NaCl, 5 mM $MgCl_2$ and 0.5 mg/mL bovine serum albumin (BSA) for 1 h at 4°C. The mixture was incubated overnight with the antibody-bound protein G sepharose at 4°C. The immunoprecipitates were washed with wash buffer (20 mM HEPES, pH 7.4, 120 mM NaCl, 5 mM EDTA, 1% Triton X-100, protease inhibitor cocktail) and eluted by 2% SDS sample suffer with boiling for 5 min. The eluate was probed by rabbit polyclonal anti-hSOD1 antibody.

In vitro ubiquitination assay

In vitro ubiquitination assay was performed as previously described with minor modifications (Hatakeyama *et al.* 2001). A 1 μL aliquot of 10 μM bovine Hsc70 was reacted with E1 (100 nM), E2 (ubcH5a; 1 μM), 0.4 μg/μL HA-ubiquitin and 1 μL 10 μM His-CHIP in the ubiquitination assay buffer (20 mM Tris-HCl pH 7.5, 10 mM KCl, 2 mM ATP, 2 mM phosphocreatine, 0.05 U/μL phosphocreatine kinase, 2 mM DTT and 5 mM $MgCl_2$) at a volume of 20 μL for 30 min at 37°C. The reaction was terminated by adding 4% SDS sample buffer for 5 min at 95°C. Polyubiquitination was evaluated by western blotting using antibodies against the substrates and HA (3F10; Roche).

Degradation assay

Neuro2a cells were transiently transfected with SOD1-FLAG and HA-ubiquitin with or without CHIP. At 12 h after transfection, cells were treated with 10 μg/mL cycloheximide (CHX) to prevent protein synthesis, and were harvested 0, 6 and 24 h after CHX treatment by denaturing buffer with boiling for 5 min. The same volume of lysates was analyzed by western blotting using anti-FLAG antibody. The remaining SOD1-FLAG was quantified by densitometry using Scion Image software. Using this method, we confirmed that wild-type SOD1-FLAG was stable until 24 h after CHX treatment, whereas mutant SOD1-FLAG proteins were more rapidly degraded. This degradation was reversed by proteasome inhibitor (data not shown). These data were the same as those from a pulse-chase experiment reported previously (Johnston *et al.* 2000).

Assay for interaction of ubiquitinated Hsp/Hsc70 with mutant SOD1

We investigated the interaction of mutant SOD1 with ubiquitinated Hsp/Hsc70 by the following two methods. In one experiment, Neuro2a cells were transiently transfected with SOD1-FLAG and HA-ubiquitin, and cell lysates were immunoprecipitated by anti-FLAG affinity gel. The immunoprecipitates were washed in ATP-containing buffer (10 mM ATP, 20 mM Tris-HCl pH 7.5, 100 mM NaCl, 5 mM $MgCl_2$ and protease inhibitor cocktail) for 15 min at 37°C with gentle shaking (ATP wash). The affinity gel was then washed three times in RIPA buffer and the eluate was assayed by western blotting using antibodies against Hsp/Hsc70 and HA.

In a separate experiment, we employed sequential immunoprecipitation of mutant SOD1-interacting protein. Cell lysates of Neuro2a transfected with SOD1-FLAG, Hsp70-V5 and HA-ubiquitin were immunoprecipitated by anti-FLAG affinity gel; the beads were subsequently incubated in the denaturing buffer described above for 5 min at 95°C. The eluate was diluted 10-fold with dilution buffer and sequentially immunoprecipitated by anti-V5 antibody with protein G sepharose at 4°C overnight. The beads were eluted by 2% SDS sample buffer, and the eluate was analyzed by western blotting using anti-HA antibody.

Multiubiquitin-proteasome binding assay

The S5a component of the 19S complex in the 26S proteasome is a non-specific multiubiquitin binding site (Walters *et al.* 2002). Human S5a cDNA was cloned from a polyA-linked cDNA pool from a human cell line (SH-SY-5Y) by conventional PCR protocols. The primer pair used GCCGAATTCAAGATGGTGTTGGAAAGCACTA as the forward primer and GCCCTCGAGTCACTTCTTGTCTTCCTCCTT as the reverse. The PCR product was digested by EcoRI/XhoI and subcloned into pcDNA3 which was then modified to contain the FLAG tag sequence at the 5′ side of the multiple cloning sites. After verification by sequencing, the FLAG-S5a construct was subcloned into pET28a(+) at a HindIII site. Recombinant FLAG-S5a protein was induced by Isopropyl-b-D-thiogalactopyranoside (IPTG) by the protocol described above, and immunopurified using anti-M2 FLAG affinity gel (Sigma). After termination of *in vitro* ubiquitination of Hsc70 and CHIP in a 20 μL reaction mixture as described above, 80 μL 40 mM Tris-HCl (pH 7.4) were added to the reaction mixture and then inserted into a column containing FLAG-S5a. The reaction mixture was incubated for 1 h at 4°C; the column was then washed four times in RIPA buffer and eluted with 2% SDS sample buffer. Samples were immunoblotted using anti-HA antibody.

Primary spinal cord culture

Primary dissociated cultures from embryonic mouse spinal cord were prepared as described elsewhere (Urushitani *et al.* 2002). Cultures were assayed 7–8 days after plating. For immunocytochemical analysis, cultures were fixed with 4% paraformaldehyde (PFA) and were reacted with antibodies against CHIP (× 1000), NeuN (Chemicon, Temecula, CA, USA; ×500), glial fibrillary acidic protein (GFAP; Dako Glostrup, Denmark) and SMI32 (Steinberger monoclonals, Baltimore, MA, USA). Alexa 448 or 546 (Molecular Probes, Eugene, OR, USA) were used as secondary antibodies. Cultures were observed under a confocal laser microscope (Olympus; Tokyo, Japan).

Immunohistochemistry of mice

The transgenic mouse line expressing the mutant B6SJL-TgN[SOD1-G93A]1Gur^{dl} was purchased from Jackson Laboratories (Bar Harbor, ME, USA). Mouse genotypes were determined by PCR as previously reported (Gurney *et al.* 1994). Post-symptomatic transgenic mice at the age of 8 months were killed and perfusion fixed by 4% PFA. Fixed-frozen sections of the spinal cord were prepared for immunohistochemistry using affinity-purified rabbit antibody against CHIP (1 μg/mL) and polyclonal antibodies to ubiquitin (× 500; Dako, Glostrup, Denmark) and to hSOD1 (× 1000; StressGen). Primary antibodies were visualized by the avidin-biotin-immunoperoxidase complex (ABC) method using the appropriate Vectastain ABC kit (Vector Laboratories, Burlingame, CA, USA) and 3.3′-diaminobenzidine tetrahydrochloride (DAB; Nacalai Tesque, Kyoto, Japan). The experiments were performed in accordance with the RIKEN Guide for Animal Care for Research Use.

Results

Hsp/Hsc70 interacts with apo- or monomerized SOD1

Mutant SOD1 interacts with Hsp70 under heat-shocked conditions in Neuro2a cells stably expressing hSOD1 (Okado-Matsumoto and Fridovich 2002), and detergent-insoluble mutant SOD1 is co-immunoprecipitated with Hsp70 (Shinder *et al.* 2001). As shown in Fig. 1a (1), the antibody against both Hsp and Hsc70 recognized a molecule

co-immunoprecipitated with mutant, but not with wild-type, SOD1 in Neuro2a cells (Fig. 1a). Since the expression of inducible Hsp70 was very low (data not shown) under normal conditions, the main binding partner of mutant SOD1 appeared to be Hsc70. Since the binding manner of Hsp70 with mutant or wild-type SOD1 was not affected by the addition of FLAG-tag (Fig. 1a, 2), most of the experiments in this study were performed using carboxy-terminally FLAG-tagged SOD1 (SOD1-FLAG) proteins.

We next investigated the molecular features of mutant SOD1 that are recognized by Hsp/Hsc70. Mutant SOD1 is reported to take several abnormal conformations including non-native oligomers (Johnston *et al.* 2000), detergent- insoluble species (Shinder *et al.* 2001) and oxidative stress-induced aggregation (Urushitani *et al.* 2002). To evaluate the molecular size of mutant SOD1 recognized by Hsp/Hsc70 *in vivo*, detergent-soluble fractions of neuro2a cells transfected with SOD1-FLAG and Hsp70-V5 were immunoprecipitated using anti-V5 antibody. The immunoprecipitates were incubated in a 0.5% SDS sample buffer without 2ME at 37°C, and were separated in partially denaturing PAGE. Figure 1(b) shows that a considerable amount of SOD1 dimer is preserved under these conditions (lanes 2–5 in the 5% input samples). However, most of the immunoprecipitated SOD1 with Hsp70 was monomeric mutant SOD1 [lanes 3 and 4 in the immunoprecipitation (IP) samples]. For further analysis, recombinant SOD1-FLAG proteins were demetallated, remetallated, or treated with DTT or H_2O_2, and were separated in partially denaturing SDS-PAGE. Figure 1c (1) indicates that increasing concentrations of DTT shifted recombinant SOD1 protein from dimer to monomer (Fig. 1c, 1: lanes 2–5, 9–12), which is consistent with a previous report (Tiwari and Hayward 2003). On the other hand, metallation and mild oxidative conditions stabilized dimerization of SOD1 (Fig. 1c, 1: lanes 2, 6, 9 and 13). A considerable amount of monomer is found in apo-state SOD1, as is shown in lanes 1 and 8 (arrowheads). Under extreme oxidative conditions, aggregate formation was facilitated (Fig. 1c, 1: lanes 7 and 14). Next, *in vitro* binding experiments between these recombinant SOD1-FLAG proteins and bovine Hsc70 revealed that Hsc70 interacted with DTT-treated or apo-SOD1-FLAG proteins in both wild-type and mutant (Fig. 1c, 2: lanes 1, 5, 6 and 10). We could not detect an obvious interaction between Hsc70 and holo-SOD1-FLAG or H_2O_2-treated SOD1-FLAG (Fig. 1c, 2: lanes 2–4 and 7–9). These results indicate that Hsp/Hsc70 favorably interacts with mutant SOD1 by targeting either a nascent monomer before metallation or a monomerized SOD1 in a reducing environment.

CHIP interacted with and promoted the degradation of mutant SOD1

The carboxyl terminus of Hsc70-interacting protein (CHIP) is a chaperone-dependent ubiquitin ligase (Connell *et al.* 2001; Murata *et al.* 2001; Alberti *et al.* 2002). We next tested our hypothesis that Hsp/Hsc70-CHIP is involved in the proteasomal degradation of mutant SOD1. When human SOD1 was overexpressed in Neuro2a cells, endogenous CHIP was co-immunoprecipitated with mutant SOD1, but not with wild-type (Fig. 2a). Overexpressed CHIP also interacted only with mutant SOD1 proteins (data not shown). Moreover, CHIP reduced the accumulation of detergent-insoluble mutant SOD1 in a dose-dependent manner (Fig. 2b). Degradation assay of total cell lysates revealed that CHIP reduced the remaining mutant SOD1 after protein synthesis was prevented by CHX (Fig. 2c). Both effects were reversed by the proteasomal inhibitor, lactacystin (data not shown). These results indicate that CHIP interacts with and promotes the proteasomal degradation of mutant SOD1.

CHIP does not target mutant SOD1 but its interacting proteins

To investigate whether mutant SOD1 is a substrate of CHIP, we performed an *in vivo* ubiquitination assay in which cells were solubilized in RIPA buffer, with immunoprecipitation carried out before lysate denaturing (Urushitani *et al.* 2002). In this condition, overexpression of Hsp70 or CHIP with mutant SOD1 strongly augmented the association of the polyubiquitinated species to mutant SOD1, most prominently in the presence of both Hsp70 and CHIP (Fig. 3a, upper panel). CHIP contains two functional domains: the tetratricopeptide repeat (TPR) and U box domains, which are necessary for Hsp/Hsc70 interaction and ubiquitin ligase activity, respectively. Mutant CHIP with these two domains deleted did not promote mutant SOD1-polyubiquitin complex formation (Fig. 3b). However, when the membrane was re-probed by anti-SOD1 antibody, we found mono or diubiquitinated SOD1 both in wild-type and mutants, but no polyubiquitinated SOD1 corresponding to Hsp70 or CHIP overexpression (Fig. 3a, lower panel). This was unexpected, since we had assumed mutant SOD1 was a substrate of CHIP and that immunoprecipitates consisted of polyubiquitinated mutant SOD1. These results indicate, however, that other proteins that are ubiquitinated by Hsp/Hsc70 and CHIP form complexes with mutant SOD1.

RIPA buffer still preserves appreciable non-covalent interaction as seen in mutant SOD1 and Hsp/Hsc70 (our consistent observation). Therefore, we employed an immunoprecipitation assay in which lysates were denatured by 1% SDS and boiled before immunoprecipitation to preserve only covalent binding. Under these conditions, we can detect the ubiquitination of Hsp70 by CHIP as shown in Fig. 3c (1). In contrast, no substantial effect of either Hsp70 or CHIP on mutant SOD1 ubiquitination was observed (Fig. 3c, 2; compare lane 4 with lane 6 in Hsp70 or lane 8 in CHIP), although Hsp70 and CHIP augmented the association of polyubiquitinated species with mutant SOD1 in RIPA buffer (Fig. 3c, 2; compare lanes 5, 7 and 9). On the other hand, we noted oligoubiquitination of wild-type SOD1-FLAG both in

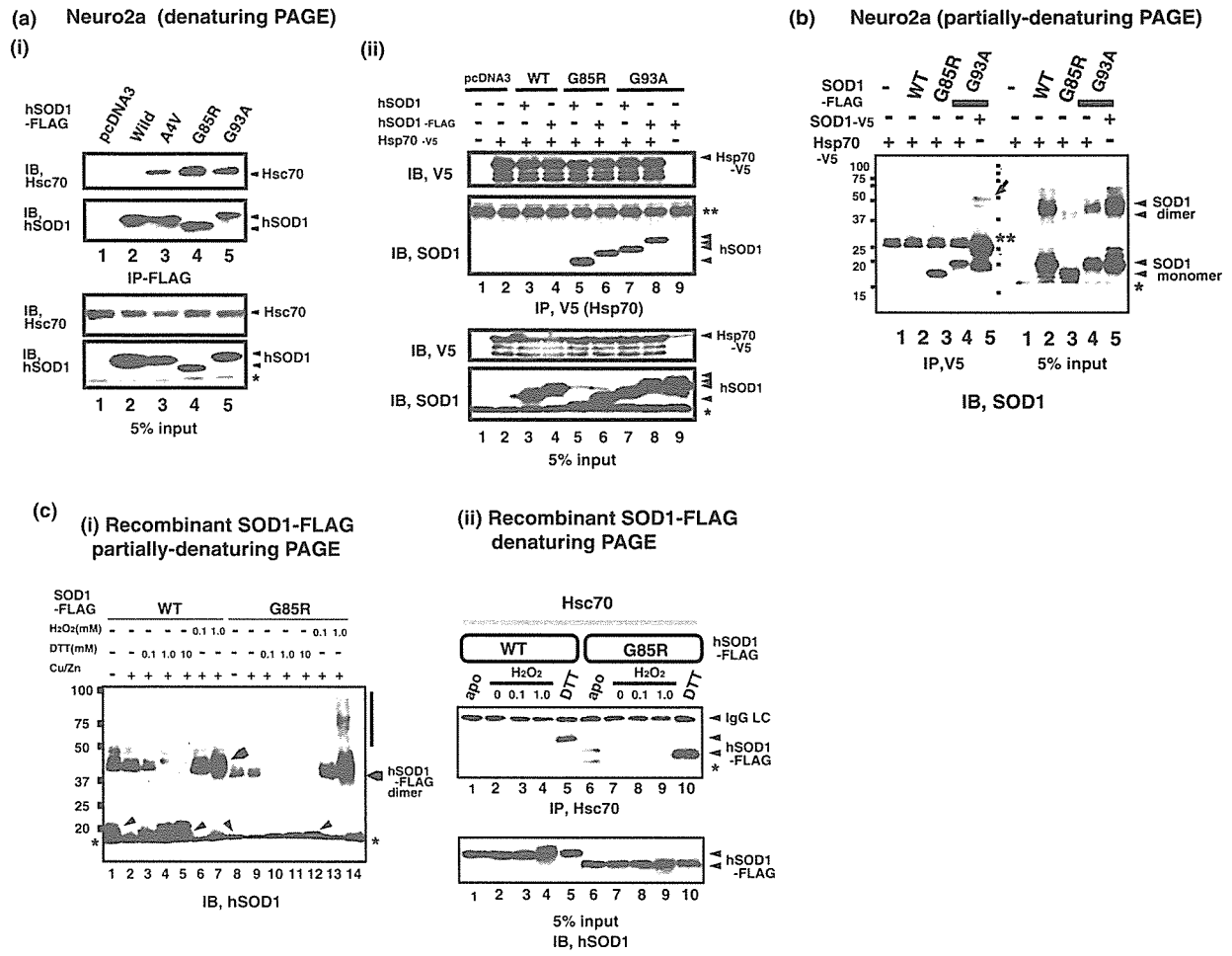

Fig. 1 Hsp/Hsc70 preferentially interacts with hSOD1 monomer or apo-state SOD1. (a) Mutant–specific interaction of SOD1 and Hsp/Hsc70 *in vivo*. (1) Neuro2a cells in 6-well culture plates were transiently transfected with hSOD1-FLAG (2 μg/well). Lysates were immunoprecipitated with anti-FLAG affinity gel, and blots were probed with anti-hSOD1 or anti-Hsp/Hsc70 antibodies. (2) Overexpressed Hsp70 interacted with mutant SOD1 with or without FLAG-tag. Neuro2a cells were transfected with Hsp70-V5, and hSOD1 with or without FLAG tag, at the C′ terminus. The cell lysates were immunoprecipitated by anti-V5 antibody, and the precipitates were probed by anti-hSOD1 or anti-V5 antibody. Asterisk indicates endogenous mice SOD1. Double asterisks indicate IgG light chain. In both (1) and (2), the immunoprecipitates were incubated in 2% SDS sample buffer containing 2ME for 5 min at 95°C before SDS-PAGE (denaturing PAGE). (b) The predominant species of mutant SOD1 that interacts with Hsp70 was a detergent-soluble monomer *in vivo*. Neuro2a cells were transiently transfected with SOD1-FLAG (1 μg/well) and Hsp70-V5 (1 μg/well) in a 6-well culture plate. The 1% TritonX 100-soluble lysates were immunoprecipitated by anti-V5 antibody. The lysates of 5% input lysates were incubated with the same volume of 1% SDS sample buffer without 2ME for 15 min at 37°C, and immunoprecipitates were eluted by 0.5% SDS sample buffer without 2ME for 15 min at 37°C. Samples were resolved in 10–20% gradient SDS-polyacrylamide gel (partially denaturing PAGE), and blots were analyzed by western blotting using anti-SOD1 antibody. Asterisk indicates endogenous mouse SOD1, and double asterisks show IgG light chain. For control in native PAGE, SOD1-V5 and SOD1-FLAG were transfected and immunoprecipitated by anti-V5 antibody. Arrow indicates dimeric SOD1 (G93A) formed by SOD1-V5 and SOD1-FLAG. (c) Apo-state or SOD1 monomer was recognized by Hsc70 *in vitro*. (1) Effect of redox conditions on dimer stabilization and monomerization. *E. coli*-purified SOD1-FLAG proteins were demetallated (lanes 1 and 8) and remetallated (lanes 2–7, 9–14). The recombinant proteins were treated with the indicated concentrations of DTT for 1 h at 37°C (lanes 3–5, 10–12) or treated with H_2O_2 for 1 h at room temperature (lanes 6 and 7, 13 and 14). The reaction mixtures were reacted with sample buffer without 2ME for 10 min at 55°C, and were resolved in 10–20% gradient SDS-polyacrylamide gel (partially denaturing PAGE). The blot was probed by anti-SOD1 antibody. Arrows indicate dimeric SOD1, whereas arrowheads indicate the reduced form of monomeric SOD1. These are present in lanes 3–5 in the wild-type, and 10–12 in G85R. In lanes 1, 7, 8 and 14, the amounts of monomeric SOD1-FLAG proteins increased (arrowheads). The asterisk indicates a possibly non-reduced monomeric SOD1. (2) *In vitro* binding experiment showing the interaction of demetallated or monomerized mutant SOD1-FLAG with Hsc70. Recombinant SOD1-FLAG proteins that were demetallated, remetallated, or treated with H_2O_2 (0.1 or 1.0 mM) or DTT (1 mM), were incubated with bovine Hsc70, followed by immunoprecipitation using anti-Hsp/Hsc70 antibody and western blotting using anti-SOD1 antibody. The asterisk indicates possible degradation product of SOD1 protein under apo-state or reducing environment.

RIPA buffer and denaturing buffer (arrowhead). To confirm this, Neuro2a cells were transfected with HA-ubiquitin and hSOD1, with or without FLAG tag, followed by immunoprecipitation using anti-HA antibody and western analysis using anti-SOD1 antibody. As shown in Fig. 3c (3), wild-type SOD1 appeared to be oligoubiquitinated to the same extent as mutant SOD1, irrespective of FLAG tag. These results strongly indicate that CHIP promotes proteasomal degradation of mutant SOD1 by ubiquitination of its binding partners.

Mutant SOD1-associated Hsp/Hsc70 was ubiquitinated and interacted with 26S proteasome subunit

Since CHIP did not ubiquitinate mutant SOD1 despite promoting mutant SOD1 degradation, it is possible that the ubiquitination of Hsp/Hsc70 was involved in proteasomal degradation of mutant SOD1. To test this, we first employed an ATP wash of co-immunoprecipitates containing mutant SOD1 from cell lysates to remove attached Hsp/Hsc70. The wash of the precipitates in ATP containing buffer at 37°C released Hsp/Hsc70 together with substantial ubiquitinated species (Fig. 4a, 1). Next, we proved directly that mutant SOD1-associated Hsp70 was ubiquitinated by sequential immunoprecipitation. The lysates from Neuro2a cells transfected with SOD1-FLAG, Hsp70-V5 and HA-ubiquitin were immunoprecipitated with anti-FLAG antibody, and then by anti-V5 antibody, sequentially. As shown in Fig. 4a (2), mutant SOD1-associated Hsp70 bound covalently with HA-tagged ubiquitin. Since a polyubiquitin chain is the recognition signal for ubiquitinated molecules to be delivered to 26S proteasome, we investigated whether polyubiquitinated Hsp/Hsc70 might translocate mutant SOD1 by S5a co-immunoprecipitation assay using recombinant proteins. S5a is a subunit of 26S proteasome that interacts with the polyubiquitin chain (van Nocker *et al.* 1996). First, we performed an *in vitro* ubiquitination experiment to make CHIP ubiquitinate Hsc70. CHIP also autoubiquitinates (Fig. 4b, 1). Next, the reaction mixture was incubated with recombinant FLAG-S5a subunit and was immunoprecipitated with anti-FLAG. As shown in Fig. 4b (2), a polyubiquitinated species, assumed to be Hsc70, interacted with the S5a subunit. This interaction was polyubiquitin-specific because no mono-ubiquitin (arrowhead), monoubiquitinated Hsc70 (arrow) or CHIP (double arrow heads) were observed as clearly as polyubiquitin. However, mutant SOD1 was not detected in this assay because the reaction buffer of the *in vitro* ubiquitination experiments contained ATP and $MgCl_2$, which may have had similar effects as the ATP wash (data not shown).

Neuron-specific distribution of CHIP and its co-localization with mutant SOD1-containing aggregates in the spinal motor neurons from end-stage hSOD1^{G93A} mice

CHIP mRNA was originally reported to be most abundant in skeletal muscle and heart, with somewhat lower expression levels in pancreas and brain tissue (Ballinger *et al.* 1999). In the present study, CHIP was exclusively expressed in neurons in primary mouse embryonic spinal cord culture in which approximately 90% of CHIP-positive cells were merged with the neuronal marker anti-NeuN (Fig. 5a, 1–3), but not with anti-GFAP antibody (Fig. 5a, 7–9). Motor neurons, identified by SMI32-positivity and their characteristic shape, also expressed CHIP (Fig. 5a, 4–6). The surviving motor neurons in the mutant SOD1-related ALS patients or mouse models display ubiquitinated SOD1-immunopositive inclusions, designated Lewy body-like hyaline inclusions (LBHI) (Kato *et al.* 1997). Therefore, we examined whether LBHIs in the spinal cord sections from symptomatic hSOD1^{G93A} transgenic mice immunostained with CHIP antibody (Fig. 5b, 1–3). Immunohistochemistry revealed that LBHIs are frequently immunostained by anti-CHIP antibody (Fig. 5b, 4 and 5), as well as by anti-ubiquitin (Fig. 5b, 2) and anti-SOD1 (Fig. 5b, 3) antibodies. These results suggest that CHIP is involved in the formation of LBHIs in the motor neurons of mutant SOD1 transgenic mice.

Discussion

In the present report, we demonstrated the roles of Hsp/Hsc70 and CHIP in degradation of mutant SOD1 at the proteasome. Hsp/Hsc70 preferentially interacted with the apo-state, or monomeric form, of mutant SOD1. CHIP promoted the degradation of mutant SOD1 at the proteasome in a chaperone-dependent manner. Surprisingly, this effect was mediated by polyubiquitination of Hsp/Hsc70, not mutant SOD1. Hence, we proposed a novel cascade for mutant SOD1 metabolism as shown in Fig. 6. Although Hsp/Hsc70 attempts to fold nascent monomeric SOD1, this function may be less effective in mutant SOD1 than in wild-type. Accordingly, the Hsp/Hsc70 may be ubiquitinated by its ubiquitin ligase including CHIP, resulting in recruitment of mutant SOD1 to the proteasome. Along with proteasomal impairment (Urushitani *et al.* 2002), the polyubiquitin complex may result in the formation of pathological aggregate, a hallmark of ALS.

Hsp/Hsc70 and mutant SOD1 monomers

Hsc70 was shown to recognize the apo-state or DTT-treated form of SOD1 protein (Fig. 1c, 2). The fact that mutant SOD1 is monomerized and destabilized by reducing agents, whereas wild-type is not, indicates that the SOD1 monomer is a key molecule underlying the diverse pathological conditions seen in mutant SOD1-linked pathology (Tiwari and Hayward 2003). Apo-state SOD1 is also implicated in mutant SOD1-linked pathogenesis. For instance, apo-SOD1, in both wild-type and mutant forms, appears to enter into mitochondria (Okado-Matsumoto and Fridovich 2002). Physiologically, a proportion of wild-type SOD1 exists as a homodimeric apoenzyme *in vivo*, although apo-state SOD1 is more readily

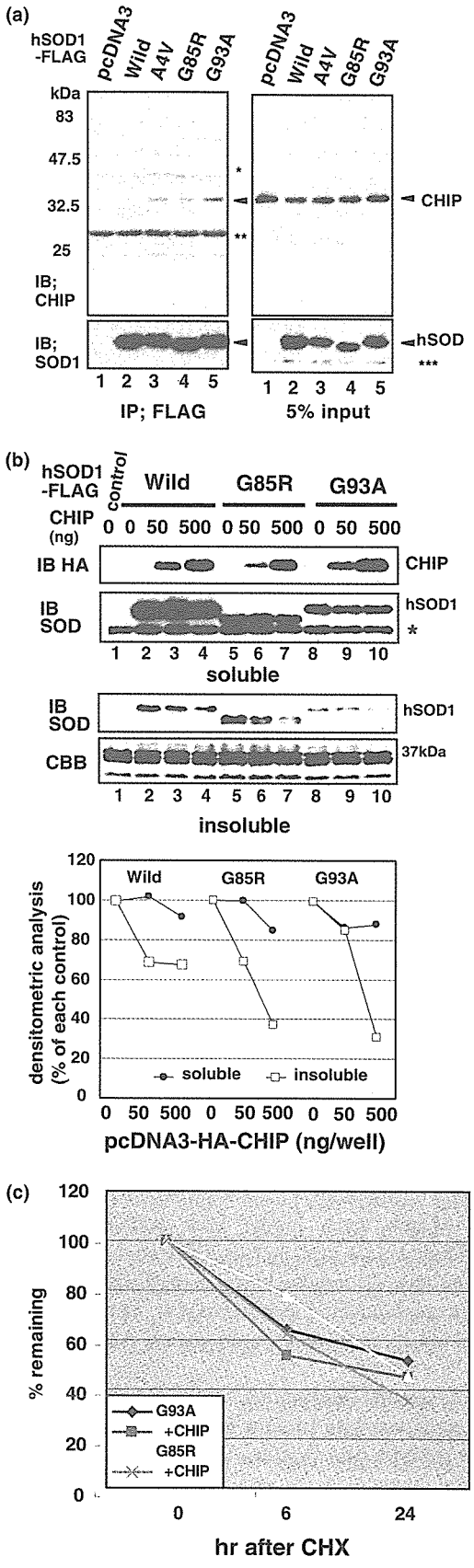

Fig. 2 CHIP interacts with and promotes ubiquitin complex formation of mutant SOD1. (a) Interaction of overexpressed mutant SOD1 with endogenous CHIP *in vivo*. Neuro2a cells in 6-well culture plates were transiently transfected with hSOD1-FLAG (2 μg/well). Lysates were immunoprecipitated with anti-FLAG affinity gel and blots were probed with antibodies against CHIP and hSOD1. Single and double asterisks indicate IgG heavy and light chains, respectively. (b) CHIP degraded misfolded mutant SOD1 in a dose-dependent manner at proteasome. Neuro2a cells in 12-well culture plates were transiently transfected with hSOD1-FLAG (1 μg), together with HA-CHIP at the indicated concentrations (total DNA, 1.5 μg/well). Supernatant (soluble) and pellet (insoluble) fractions in TritonX 100-containing buffer were immunoblotted using anti-HA or anti-SOD1 antibody. Immunoblots were analyzed by densitometry, and each value was expressed as the percentage of vector control in each genotype. Coomasie brilliant blue (CBB) staining of the insoluble fraction showed that an equal amount of protein was analyzed in each lane. The asterisk indicates endogenous mouse SOD1. (c) CHIP promotes degradation of mutant SOD1. Neuro2a cells in 12-well culture plates were transiently transfected with SOD1-FLAG (G85R and G93A, 1 μg/well) with or without HA-CHIP (0.5 μg/well). At 16 h after transfection, cells were treated with CHX (10 μg/mL) to prevent protein synthesis. Cells were harvested immediately (0), 6 and 24 h after CHX treatment and solubilized in denaturing buffer with boiling for 5 min. Remaining SOD1-FLAG proteins were probed by anti-FLAG antibody, and scanned images were analyzed by densitometry. Each data value represents percentage of remaining SOD1-FLAG compared with the one immediately after CHX treatment.

monomerized than holoenzyme by non-denaturing SDS-PAGE (Bartnikas and Gitlin 2003). Moreover, recent data show that apo-state wild-type SOD1 and metal-deficient mutant SOD1 form a β-sheet structure that mimics amyloid β fibrils (Elam *et al.* 2003; Strange *et al.* 2003). Our data showing that Hsc70 interacts with this reportedly pathogenic SOD1 strongly suggests that this reaction plays a fundamental role in mutant SOD1 metabolism and pathology *in vivo*. In particular, the evidence that overexpressed Hsc70 interacts with soluble SOD1 allows us to hypothesize about another potentially beneficial role for Hsp/Hsc70 in mutant SOD1 metabolism in addition to the refolding of aggregated SOD1. Unexpectedly, Hsc70 did not interact with oxidized SOD1 as tightly as with apoenzyme or monomerized SOD1 (Fig. 1c, 2). One explanation for this phenomenon may be that oxidative conditions stabilized the intramolecular disulfide bond of SOD1 and supported its dimerization. Alternatively, aggregates or fragments formed by H_2O_2 may interact with one another and trap hydrophobic residues inside the aggregates.

The role of Hsp/Hsc70 and CHIP in mutant SOD1 degradation

Hsp70 is known to accelerate the proteasomal degradation of androgen receptors with abnormally expanded polyglutamine (Bailey *et al.* 2002; Adachi *et al.* 2003). CHIP may be involved in this metabolism since CHIP reportedly promotes the ubiquitination of wild-type androgen receptors (Cardozo